

Geology and new mineralization in the Joss'alun belt, Atlin area

Mitch Mihalynuk¹, Lee Fiererra², Steve Robertson³,
Fionnuala A.M. Devine⁴ and Fabrice Cordey⁵

Introduction

In 2002, Ministry of Energy and Mines personnel discovered copper mineralization approximately 75 km south southeast of Atlin while conducting a regional geological mapping program as part of the federal and provincially funded Targeted Geoscience Initiative. Following a press release (Mihalynuk, 2002), several parties staked ground in the belt. Subsequently, Imperial Metals Corporation consolidated interests and is now the key operator and tenure-holder in the area. The claim group is referred to as the NAK property and the principal mineralized zone is the Joss'alun massive sulphide occurrence.

As part of a public-private partnership agreement with Imperial Metals Corporation (henceforth referred to as "Imperial"), approximately three weeks of field mapping was conducted in 2003 in the belt of rocks containing the mineralization to clarify geological relationships. An additional 1.5 weeks on reconnaissance geological mapping was aimed at outlining more regional exploration targets. Operational funding was provided by Imperial.

This report is based upon the results of mapping conducted on the claim blocks owned or optioned by Imperial (NIC, KNACK, WACK, Dark and D1 to D12). In addition, we report here on results of mapping and sampling outside of the claim blocks, and a brief synopsis of drill results and property exploration. Highlights include:

- discovery of new mineralization within the belt of rocks containing the Joss'alun occurrence, extending the mineralized belt about 2.5 km northwest and 5 km southeast of the Joss'alun;
- intersections in two drill holes at the Joss'alun that assayed 0.94% copper over 17.75 metres and 0.34% copper over 53.45 metres;

- lithochemical data that points to a forearc or back-arc setting for the unit hosting mineralization;
- recognition of Paleozoic-Mesozoic stratigraphy that appears to have regional application, including an extensive ferruginous chert horizon, locally copper stained, that is probably of Early Permian age; and
- synthesis of a regionally applicable structural history that includes an episode of extension, possibly back arc basin extension, with implications for volcanogenic and sedimentary-exhalative (VMS/SEDEX) mineralization.

Access and Previous Work

Access to the NAK property is most effectively achieved using a helicopter charter based out of Atlin, 75 kilometres to the north-northwest. One large lake about 7.5 km north northwest of the Joss'alun occurrence, informally known as Windy Lake, is large enough to accommodate a floatplane - so long as loaded departures are not required. There are no all-season roads within the area. One rough, fire abatement road extends to Kuthai Lake, about a 2.5-hour drive from Atlin, and about 30 km northwest of the NAK property. It is suitable for four wheel drive or all-terrain vehicles and requires fording the O'Donnell River and Dixie Lake outflow. Around the NAK property, travel by foot is relatively easy, except for some steep mountainsides around Hardluck Peaks. The proposed access road to the Tulsequah Chief mine is, at its closest point, 22 km from the NAK property.

Previous regional map coverage of the NAK area is of early to mid 1950s vintage (Aitken, 1959), pre-dating the advent of plate tectonics. Thematic revision mapping in the mid to late 1960's by Monger (1969, 1975) covered much of the carbonate-dominated rocks north and east of the NAK property. Monger (1975) pieced together a biostratigraphy and used igneous geochemistry, map relationships, and the recognition of a disrupted ophiolitic succession to show that the Atlin area is composed largely of relict ocean basin crust and oceanic islands. Terry (1977) confirmed this assertion and suggested an analogue in the Pindos ophiolites of Greece. Ash (1994) drew similar conclusions from the ophiolitic ultramafic rocks near the town site of Atlin. A more extensive geochemical and petrogenetic study by English *et al.* (2002) shows that the most common mafic volcanic rocks in the region formed within a primitive island arc setting.

¹ Geoscience, Research and Development Branch, Ministry of Energy and Mines, Victoria, BC

² University of Victoria, Victoria, BC. Current affiliation: Imperial Metals Corporation, Vancouver, BC

³ Imperial Metals Corporation, Vancouver, BC

⁴ Imperial Metals Corporation. Current affiliation: Department of Earth Sciences, Carleton University, Ottawa, ON

⁵ PaléoEnvironnements & PaléobioSphere, Université Claude Bernard, Lyon, France



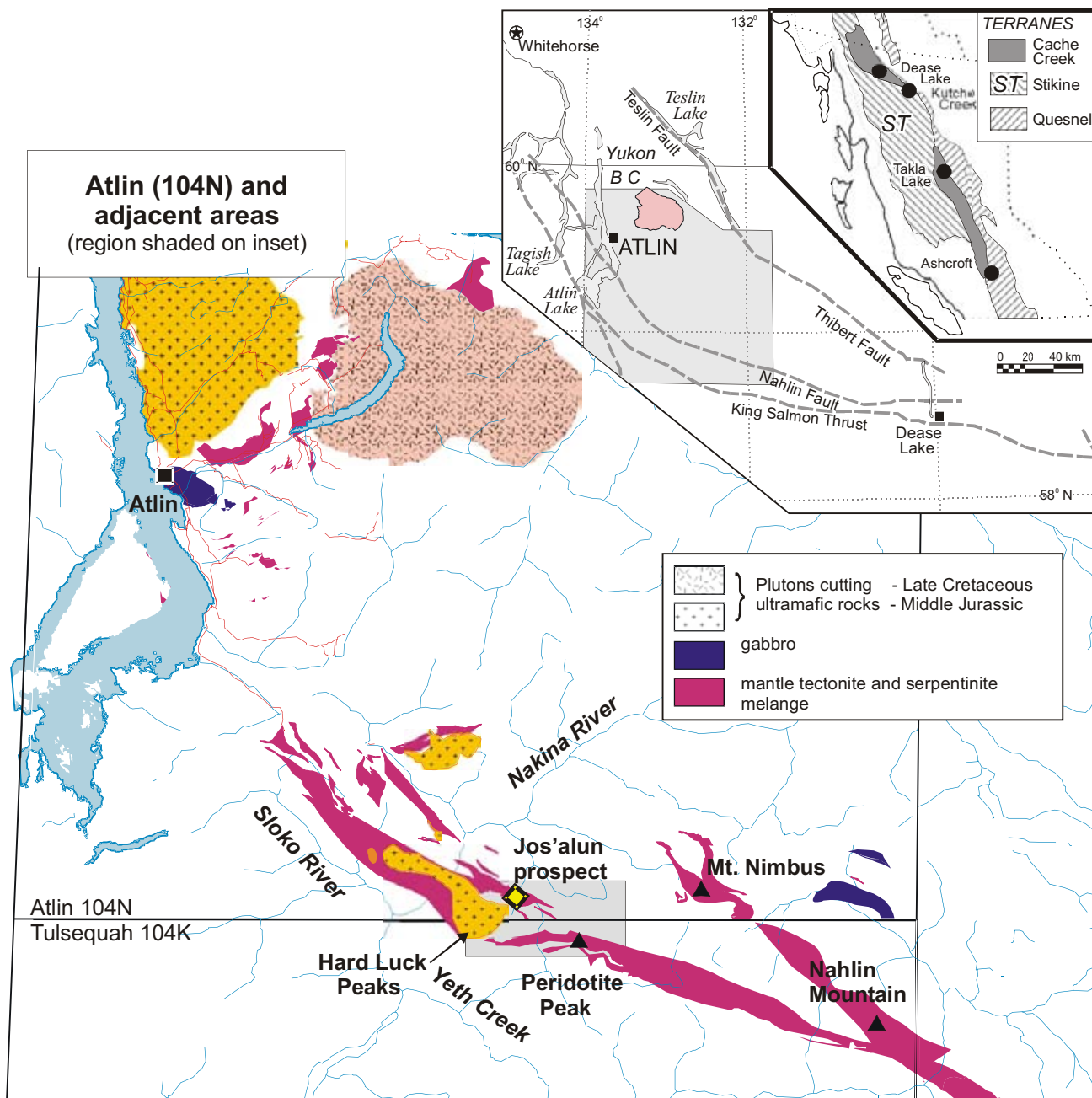
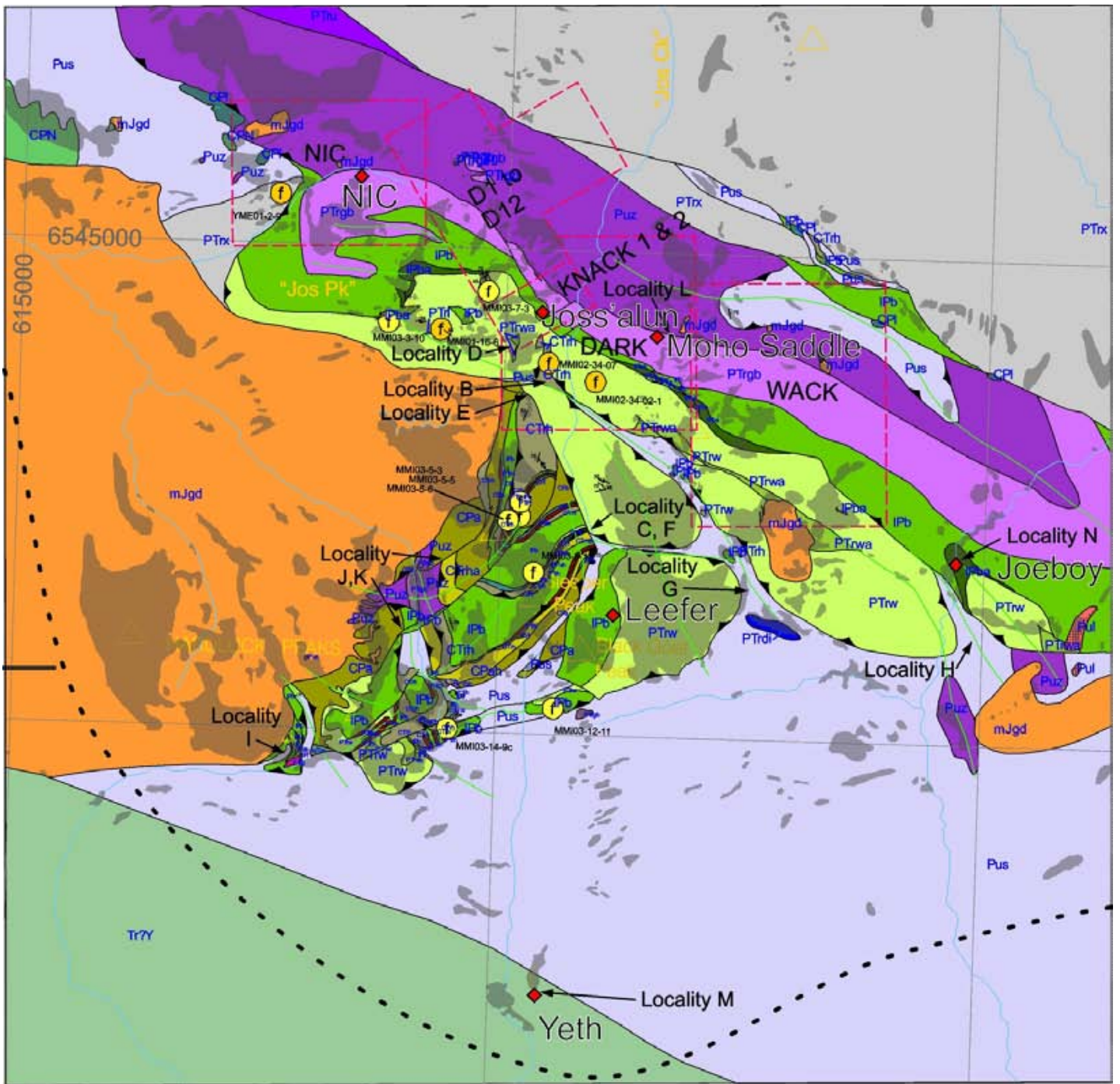


Figure 1. Location of the NAK property. Geology after Mihalynuk *et al.* (1996, 2003a, b) shows the Nahlin ultramafic body and other mantle rocks, and major intrusive bodies. Location of Figure 2 is shaded on the map. The region covered by the map is shown shaded on the inset figure of British Columbia.

In 1996, a compilation of Atlin geology was completed as part of a provincial mineral potential evaluation (Mihalynuk *et al.*, 1996). This map has been corrected and recompiled by Massey *et al.* (2003); it is available for viewing or download at <http://www.em.gov.bc.ca/Mining/Geosurv/Publications/>. In 1978 a Regional Geochemical Survey (RGS) was conducted over the entire Atlin 1:250 000 sheet (BCMCM, 1978). Archival stream sediment samples were reanalysed for a broader range of elements, including gold, and published in 2000 (Jackaman,

2000; available for download at [www.em.gov.bc.ca/Mining/Geosurv/rgs/sheets/104n .htm](http://www.em.gov.bc.ca/Mining/Geosurv/rgs/sheets/104n.htm)). In the same year, a regional aeromagnetic survey of the entire Atlin map sheet, about 14 000 square kilometers, was conducted (e.g. Dumont *et al.*, 2001). Mapping at 1:50 000 scale across a transect of the southern Atlin mapsheet (104N/1, 2 & 3) was begun in 2001 as part of the two-year, Federal and Provincially-funded Targeted Geoscience Initiative (TGI). Results of TGI mapping have been published by Mihalynuk *et al.* (2002, 2003a and references therein). Three 1:50 000



Intrusive Rocks

- mJgd Middle Jurassic hornblende-biotite granodiorite
- PTrg Permo-Triassic? foliated quartz-feldspar prophyry
- PTrgb Permo-Triassic gabbro
- PTwa gabbro to quartz diorite as knockers

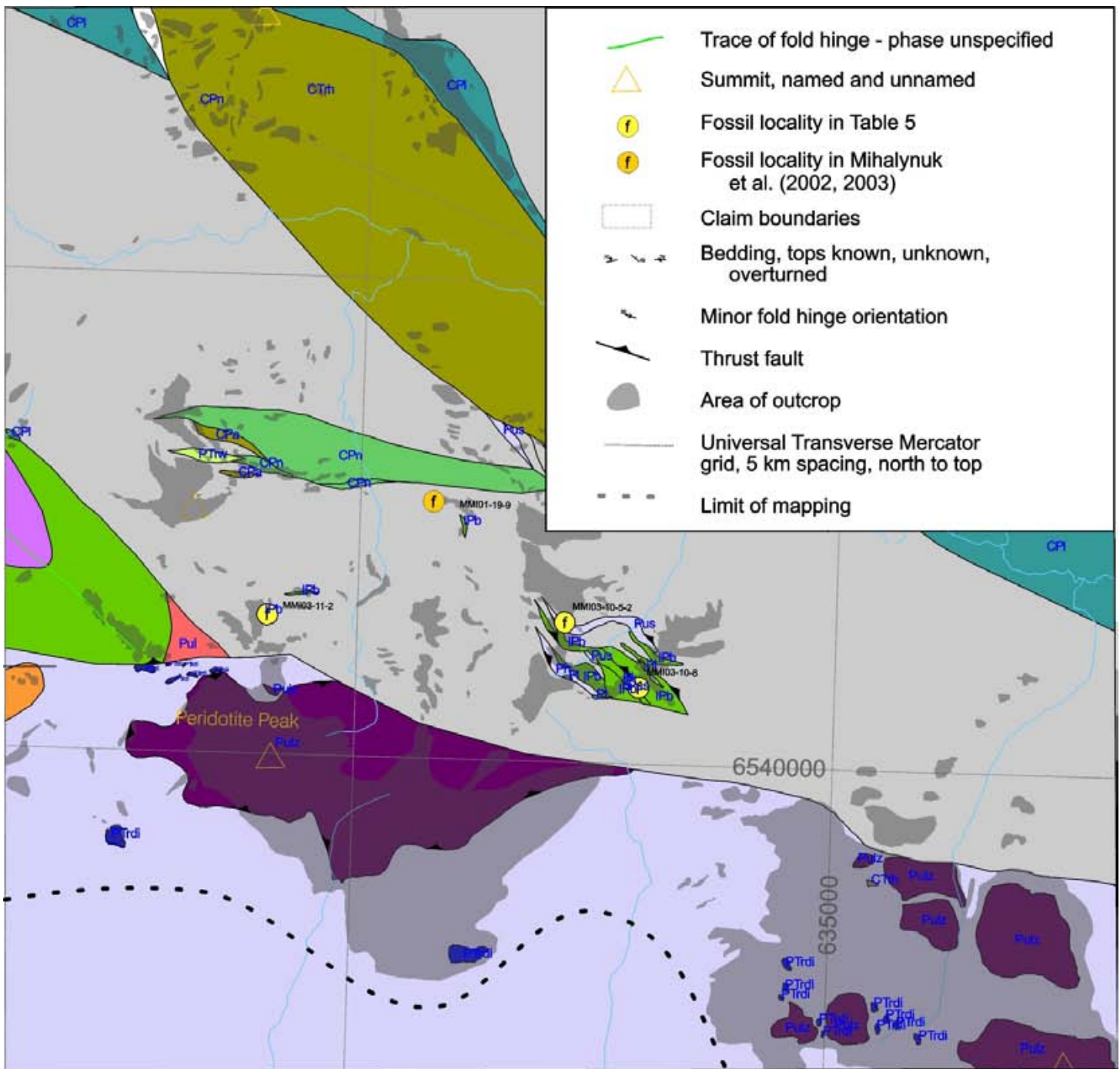
Mantle Rocks

- mainly ?Triassic to Permian
- Pus serpentinite - mainly after harzburgite and listwanite-altered equivalent
 - Puz harzburgite tectonite
 - Puz tectonized lherzolite

Volcanic & Sedimentary rocks

- PTx Permian to Mid-Jurassic accretionary complex, chert>>basalt<<wacke>>carbonate~ultramafite
- mITrs Middle- Upper Triassic blue-grey cherty volcanic siltstone
- CTth Middle Triassic grey ribbon chert
- Tr?Y ?Triassic Yeth Creek formation

Figure 2. Simplified geology of the Joss'alun belt in the Nakina River area (BC Geographic Survey sheets 104K.096N, 097N and 104N.006S, 007S. Geology is based upon published mapping by Mihalynuk et al. (2002, 2003a, b) and regional geology of Aitken (1959) and Souther (1971).



- | | | | |
|-------------|--|------------------|---|
| PTw | Late Permian to Early Triassic Hardluck fm. -conglomeratic, quartz-rich clastics | IPa | Mainly Permian to Triassic basaltic agglomerate |
| PTwa | Hardluck formation -argillite ±siltstone, sparse laminated volcanic siltstone | IPb / CPN | Mainly Permian to Triassic basalt volcanoclastic>pillows |
| PTx | Permian to Triassic accretionary complex; chert>>basalt><wacke>carbonate | CPa | Carboniferous to Permian chert and cherty argillite |
| CPI | Mainly Permian to Triassic limestone, minor interbedded chert | CPI | Carboniferous to Permian limestone, locally fusulinid packstone |
| PTxa | Ferruginous chert, well-bedded | CTth | Carboniferous to Permian argillite > fine wacke |

Unpublished mapping by Canil and Johnston (2004) is presented in the southeastern corner (Peridotite Peak and ultramafic rocks to the southeast).

scale geological maps that cover the transect area will be published in the near future.

Mineral exploration work around the Joss'alun discovery has been carried out by Imperial Metals Corporation, included geophysical and geochemical surveys, culminating in a diamond drill program which was concluded in the autumn of 2003.

Regional Geological Setting

Rocks comprising the belt that hosts the Joss'alun occurrence can be broadly separated into three distinct packages. From oldest to youngest they are: Mississippian to Early Jurassic Cache Creek oceanic rocks; coarse, quartz-rich clastic strata of probable Late Permian to Triassic age; and Middle Jurassic, post-tectonic intrusions, like the Nakina River stock.

Southwest of the NAK property, the Cache Creek rocks are bounded by the crustal-scale Nahlin fault that marks the contact with Lower to Middle Jurassic strata of the Laberge Group. All rocks older than the ~172 Ma Jurassic plutons have been folded and faulted, most recently by southwest-verging folds and thrusts, that formed between 174 and 172 Ma (Mihalynuk *et al.*, 2004). Discreet high angle faults cut plutons south of the map area that are as young as Eocene (Mihalynuk *et al.*, 1995).

Nak Stratigraphy

In a gross sense, a mantle to supracrustal architecture can be recognized in the NAK area, and the mantle/crustal components (harzburgite/gabbro) can be treated as stratigraphic elements, originally located beneath the supracrustal strata. A description of the mantle to supracrustal components follows.

MANTLE

Mantle rocks are best exposed within the Atlin area north of the Joss'alun occurrence, where they comprise part of the Nahlin ultramafic body, a coherent 1.5 x 15 km, dun-weathering body, best exposed south of the Nakina River. At that locality, the mantle rocks are bound to the west by gabbro, which passes upwards into submarine basalt, host to massive sulphide mineralization at the Joss'alun occurrence. Mantle rocks are comprised almost entirely of harzburgite (olivine, orthopyroxene and chrome spinel), with minor dunite (olivine). To the southeast, at Peridotite Peak, lherzolite containing up to 25% bright green chromian diopside, is exposed together with the harzburgite (see Canil *et al.*, this volume). Harzburgite commonly displays a high temperature tectonite fabric (Photo 1), which results in quasiductile elongation of the pyroxene grains (e.g. both harzburgite and dunite have been subjected to varying degrees of serpentinization). Typically, only relicts of olivine persist within a serpentine matrix. Other alteration minerals include quartz-magnetite-mariposite (listwanite alteration assemblage), and chrysotile (typically as veinlets less than 5 mm thick).



Photo 1. A high temperature mantle tectonite fabric is developed in the harzburgite west of "Jos Creek".

GABBRO

Gabbro forms a relatively continuous outcrop belt along the eastern margin of the mantle section. It is composed mainly of clinopyroxene orthopyroxene, with pyroxene subequal in abundance to plagioclase. It is typically medium-grained; although locally pegmatitic, such as in the saddle northeast of the NAK camp. A conspicuous feature of the gabbro is the presence of a reticulate vein network. Petrographic work conducted on gabbro throughout the Cache Creek terrane shows these veins to be comprised mainly of prehnite quartz and calcite. In two outcrops northwest of the NAK camp, gabbro shows an intrusive contact relationship with the mantle rocks. In at least three other localities, an intrusive relationship between gabbro and the overlying mafic and hypabyssal volcanic rocks is preserved.

BASALT

Basalt exposed within the NAK area is typically green-grey, blocky-weathering and dark green on fresh surfaces. It is a relatively resistant unit and caps several ridges south and east of the Joss'alun occurrence. Three lithologies are recognized: pillowed flows, agglomerate (herein defined as a monomict volcanic unit with large lapilli or breccia-sized fragments that are commonly rounded), and varitextured tuffaceous strata that may include hyaloclastite, flow breccia, tuffite and dense flows (a grab bag of basaltic lithologies not included in the first two units).

Pillowed flows are well displayed at the Joss'alun and on the peak at the western head of "Jos valley" ("Sleeper Peak", Photo 2). Pillow basalts are fine grained, rarely containing medium-grained feldspar laths comprising up to 10% of the rock. Pillows are typically vesicular and may display zones of varying vesicle size. Rims are chilled and chlorite altered. Pillows range from 15 to 150 cm across and appropriately oriented sections may show flow tubes and clear indications of flow tops. Interpillow lime mud or, less

TABLE 1. RESULTS OF INDUCTIVELY COUPLED PLASMA MASS SPECTROSCOPY (ICPMS) ANALYSIS

Element	Mo	Cu	Pb	Zn	Ag	Ni	Co	Mn	Fe	As	U	Au	Th	Sr	Cd	Sb	Bi	V
Units	ppm	ppm	ppm	ppm	ppb	ppm	ppm	ppm	%	ppm	ppm	ppb	ppm	ppm	ppm	ppm	ppm	ppm
Detection Limit	0.01	0.01	0.01	0.1	2	0.1	0.1	1	0.01	0.1	0.1	1	0.1	0.5	0.01	0.02	0.02	2
Station Number																		
LFE03-4-1	0.05	1562.18	0.19	7.6	171	102.1	11.3	167	0.99	0.6	b.d.	490.9	b.d.	46.8	0.06	0.02	b.d.	7
LFE03-17-4	0.85	2224.89	1.35	33.3	761	29.4	35.1	444	9.52	16.8	0.1	16.2	b.d.	45.7	0.14	0.14	0.17	68
LFE-03-17-7	8.02	121.14	5.29	568.9	124	3.1	17.4	1153	6.97	15.3	b.d.	6.6	b.d.	4.4	1.85	0.38	0.55	94
STD GSB Till 99	0.78	154.01	181.02	320.2	1233	192	40.9	1259	6.17	48.2	0.4	34	3	15.7	0.62	7.76	0.21	91
MMI03-12-2	8.09	8818.62	1.59	39.7	618	10.8	126.3	879	13.29	11.1	b.d.	13.8	b.d.	2.6	0.12	0.11	0.61	144
MMI03-12-2-3	1.74	323.14	0.37	59.1	40	9.4	27.3	608	6.05	3.9	b.d.	1.1	0.1	2.6	0.09	0.12	0.09	131
MMI03-12-2-4	2.09	33008.09	1.26	36.5	1901	11.3	99.8	267	10.73	2.4	b.d.	15.8	b.d.	1.4	0.58	0.09	0.12	77
MMI03-12-2-5	0.05	13.34	0.05	17.8	7	1481.1	72	873	4.13	29.7	b.d.	10	b.d.	238.8	0.01	0.23	b.d.	18
MMI03-12-5	0.3	11.14	0.19	15.8	6	1464.6	53.8	584	3.1	48.1	b.d.	0.6	b.d.	111.5	0.01	0.9	b.d.	3
MMI03-2-11	10.78	1157.96	0.93	2283.7	251	3.5	27.7	1813	8.68	8.4	0.1	18.5	b.d.	1.8	6.63	0.11	0.55	180
Acme QC	0.09	25.46	1.11	65.7	42	23.5	13.3	797	3.91	15.9	0.1	0.3	0.3	104.8	0.14	0.14	0.02	66
MMI03-25-14	2.14	526.91	36.3	1383.3	4189	10.9	26.4	833	6.37	25	0.4	114.8	b.d.	4.6	5.79	0.85	b.d.	238
Std. GSB Till 99	0.83	161.36	186.49	333.7	1209	204.2	43.8	1317	6.43	51.8	0.4	23.2	3.1	16.3	0.65	7.42	0.22	97
MMI03-25-15b	19	480.4	316.34	733.5	2054	20.1	11.4	653	2.7	9.7	b.d.	607.5	b.d.	2.4	4.55	0.4	0.03	70
MMI03-25-5	0.17	61.54	0.28	44.4	14	61.1	25.7	618	5.21	4.3	b.d.	0.2	b.d.	4.1	0.02	0.02	b.d.	336
MMI03-25-7	0.75	177.92	13.89	241.5	584	67.8	43.8	1014	8.2	8.2	0.1	30.5	b.d.	8.5	0.76	0.1	0.05	227
MMI03-2-7	25.79	30133.98	1.66	300.4	248	29.8	317.3	1029	11.48	31.3	0.4	57.2	b.d.	0.9	0.37	0.95	0.16	137
MMI03-31-10a	0.04	33900.84	0.42	124.4	3429	163.4	62.2	502	3.22	2.6	b.d.	33.8	b.d.	2.5	0.29	b.d.	0.11	15
MMI03-31-10b	0.02	10637.51	0.79	75.3	246	84.7	63.5	447	3.27	4.1	b.d.	1	0.1	16.1	0.44	0.02	0.06	36
MMI03-31-10c	0.04	38746.7	2.86	79.2	1775	229.2	66.9	672	5.17	2.1	b.d.	1.7	b.d.	6.9	2.36	0.08	0.18	16
MMI03-31-10d	0.03	45994.16	0.81	109.4	135	322.6	108.7	1069	8.3	0.6	b.d.	2.2	b.d.	11	3.13	0.03	0.25	27
MMI03-31-12a	0.07	73665.82	1.56	61.5	4204	89.9	40.3	223	8.04	10.5	b.d.	29.9	b.d.	27.4	3.39	0.18	0.13	3
Acme QC	13.19	138.19	25.51	130.1	281	24.5	11.7	762	2.91	19.3	6.1	44.9	2.9	48	5.64	3.67	6.67	58
MMI03-31-12b	0.05	34.88	0.14	12.9	8	834.3	43.8	667	2.26	1	b.d.	b.d.	b.d.	5	0.01	b.d.	b.d.	4
MMI03-31-12c	0.05	60397.96	1.64	40.3	3192	54.3	16.9	169	6.68	1.8	b.d.	14.4	b.d.	23.3	2.44	0.11	0.05	8
MMI03-5-19-1	2.82	14981.71	3.67	87.7	6419	10.8	35.8	113	4.27	32.6	b.d.	76.4	b.d.	25.9	2.98	0.23	0.09	38
MMI03-5-19-2	0.9	9804.62	0.8	25.6	2204	5.2	8	113	1.77	4.2	b.d.	16.5	b.d.	21.2	9.25	0.04	0.03	25
MMI03-5-6	0.18	370.5	5.08	55.1	10	106.3	11	3653	1.7	0.7	0.4	0.6	1.1	20.6	0.08	0.29	0.28	15
MMI03-6-2-2	0.02	17.66	0.06	7	5	329	5.3	591	2.07	2.1	b.d.	0.2	b.d.	63	0.02	b.d.	b.d.	14
MMI03-6-5	0.86	27.16	1.89	60.3	52	5.8	8.2	505	2.47	3.5	0.1	0.6	0.1	8.1	0.09	0.6	0.06	39
MMI03-7-2	0.06	32.34	0.33	24.7	52	18.8	11.4	273	1.55	2	b.d.	b.d.	b.d.	45.1	0.03	0.05	b.d.	80
MMI03-8-7	0.13	20.56	0.38	60.3	9	13.4	16.8	767	4.14	1.7	0.2	b.d.	0.1	12	0.14	0.03	b.d.	108
MMI03-8-8	14.69	13578.54	0.75	62.7	1554	25.2	59	1128	13.97	5.6	0.1	9.9	b.d.	5.4	0.32	0.03	0.12	145
Acme QC	4.1	63.44	7.57	161.4	219	20.4	16.1	420	3.86	13.6	0.4	2.7	0.4	13.4	0.9	0.21	0.09	63
Silica blank	0.15	5.27	0.53	1.6	6	4.5	0.6	17	0.24	2.8	0.1	0.4	0.4	0.8	0.01	0.03	b.d.	7
BGR-1-001	1.56	25.02	1.48	51.4	86	26.5	60.1	559	9.01	16.9	b.d.	20.4	b.d.	10.7	0.04	0.04	0.08	59
Acme QC	12.28	137.06	23.14	128.5	264	23.3	11.5	739	2.83	18.8	5.7	39.7	2.7	45.4	5.29	3.7	5.93	57
STD GSB Till 99	0.78	154.01	181.02	320.2	1233	192	40.9	1259	6.17	48.2	0.4	34	3	15.7	0.62	7.76	0.21	91
Std. GSB Till 99	0.83	161.36	186.49	333.7	1209	204.2	43.8	1317	6.43	51.8	0.4	23.2	3.1	16.3	0.65	7.42	0.22	97
	0.805	157.685	183.755	326.95	1221	198.1	42.35	1288	6.3	50	0.4	28.6	3.05	16	0.635	7.59	0.215	94
	0.04	5.2	3.9	9.5	17.0	8.6	2.1	41.0	0.2	2.5	0.0	7.6	0.1	0.4	0.0	0.2	0.0	4.2
	4.4	3.3	2.1	2.9	1.4	4.4	4.8	3.2	2.9	5.1	0.0	26.7	2.3	2.7	3.3	3.2	3.3	4.5

Note: see Table 2 for sample locations

TABLE 1. ICPMS ANALYSES CONTINUED.

Element	Ca	P	La	Cr	Mg	Ba	Ti	B	Al	Na	K	W	Sc	Tl	S	Hg	Se	Te	Ga
Units	%	%	ppm	ppm	%	ppm	%	ppm	%	%	%	ppm	ppm	ppm	%	ppb	ppm	ppm	ppm
Detection Limit	0.01	0.001	0.5	0.5	0.01	0.5	0.001	1	0.01	0.001	0.01	0.2		0.02	0.02	5	0.1	0.02	0.02
Station Number																			
LFE03-4-1	3.9	b.d.	b.d.	113.9	1.6	93.5	0.003	2	2.89	0.016	0.01	b.d.	2.4	b.d.	0.08	b.d.	2.7	0.08	3.4
LFE03-17-4	0.83	0.019	0.5	107.2	1.16	11.8	0.175	1	1.5	0.001	0.02	b.d.	5.4	b.d.	9.46	168	13.4	0.56	5.8
LFE-03-17-7	0.57	0.031	1.1	30.6	2.02	4.5	0.128	3	2.17	0.043	0.03	b.d.	8.2	0.11	5.12	33	2.4	0.42	7.9
STD GSB Till 99	0.32	0.101	13.6	237.4	2.43	227.8	0.085	1	2.64	0.004	0.04	b.d.	14.4	0.09	b.d.	292	0.3	0.25	8.2
MMI03-12-2	0.87	0.022	1.4	59.4	2.34	1.5	0.005	2	2.24	0.004	b.d.	b.d.	8	0.17	8.82	263	25.4	1.01	10.6
MMI03-12-2-3	0.43	0.059	1.5	28.7	2.17	1.4	0.007	4	2.04	0.027	0.01	b.d.	10.4	0.23	3.31	398	1.7	0.16	9.5
MMI03-12-2-4	0.05	0.014	0.6	98.8	1.11	1.6	0.012	2	1.23	0.009	0.01	b.d.	5.3	0.09	6.49	406	46.5	0.21	6.4
MMI03-12-2-5	12.95	0.002	b.d.	441.1	9.37	34.8	b.d.	9	0.11	0.007	0.01	0.4	6.3	0.08	b.d.	4032	b.d.	0.05	0.3
MMI03-12-5	3.85	0.001	b.d.	122.8	7.17	17.7	0.002	35	0.02	0.011	b.d.	0.4	2.2	0.24	b.d.	608	b.d.	0.02	0.2
MMI03-2-11	0.21	0.045	1.6	37	1.34	2.5	0.09	1	1.91	0.026	0.02	b.d.	9.6	0.03	6.53	118	8.3	0.31	8.8
Acme QC	3.75	0.052	2.8	67.9	1.81	76.8	0.012	2	2.56	0.036	0.11	b.d.	4.9	0.02	0.12	6	b.d.	0.04	7.4
MMI03-25-14	1.17	0.033	0.6	17.5	3.67	6.2	0.383	3	3.33	0.038	0.04	b.d.	14.4	1.08	2.67	411	0.9	3.01	11.3
Std. GSB Till 99	0.34	0.107	14.4	247.6	2.55	239.4	0.09	b.d.	2.77	0.005	0.04	b.d.	14.7	0.1	b.d.	305	0.4	0.25	8.6
MMI03-25-15b	0.28	0.013	0.5	108.6	1.41	6.3	0.122	b.d.	1.21	0.025	0.05	b.d.	5.2	0.04	1.07	211	0.5	0.03	4
MMI03-25-5	1.58	0.017	b.d.	132.7	2.14	5.1	0.288	3	2.9	0.029	0.01	b.d.	5.8	b.d.	0.2	10	0.2	b.d.	9.2
MMI03-25-7	1.28	0.039	1.3	143.3	4.24	16.9	0.34	3	3.59	0.017	0.02	b.d.	16.9	0.03	2.56	415	1.4	0.03	12.5
MMI03-2-7	0.09	0.028	b.d.	47.5	2.33	2.4	0.053	1	3.61	0.003	0.02	b.d.	9.7	0.04	2.78	159	43.7	2.42	11.6
MMI03-31-10a	2.69	0.001	b.d.	159	3.13	0.9	0.012	1	3.47	0.003	0.01	b.d.	2.7	b.d.	0.89	5	30.1	1.48	4.4
MMI03-31-10b	3.4	0.019	0.9	186.5	2.46	9.7	0.044	2	3.38	0.016	0.01	b.d.	3.2	b.d.	0.34	b.d.	4.9	0.17	6
MMI03-31-10c	4.32	0.001	b.d.	296.7	2.84	1.1	0.009	1	1.87	0.007	0.01	b.d.	3.2	b.d.	2.53	8	16.4	0.41	3.6
MMI03-31-10d	5.71	0.001	b.d.	569.4	4.11	0.7	0.015	2	2.59	0.005	b.d.	b.d.	2.6	b.d.	3.6	b.d.	20.3	0.24	5.4
MMI03-31-12a	1.26	0.004	b.d.	43.5	1.11	1	0.006	1	1.31	0.002	b.d.	b.d.	0.6	b.d.	4.49	22	98.4	0.47	2
Acme QC	0.73	0.097	12.3	185.6	0.66	135.7	0.094	18	2.02	0.034	0.13	5.2	3.5	1.09	b.d.	173	4.4	0.83	6.5
MMI03-31-12b	5.64	0.001	b.d.	312.2	7.09	2.6	0.004	3	0.13	0.001	b.d.	b.d.	3.2	0.02	0.07	b.d.	0.1	b.d.	0.3
MMI03-31-12c	0.85	0.005	b.d.	63.1	1.06	0.6	0.016	b.d.	1.16	0.003	b.d.	b.d.	1	b.d.	3.3	24	74.6	0.51	1.8
MMI03-5-19-1	0.72	0.007	b.d.	88.3	0.09	0.5	0.139	1	0.47	0.001	b.d.	b.d.	2.5	0.03	3.05	467	8.4	0.23	2
MMI03-5-19-2	2.08	0.002	b.d.	79.9	0.08	b.d.	0.056	b.d.	0.4	0.001	b.d.	b.d.	1.5	b.d.	1.27	224	6.3	0.05	1.8
MMI03-5-6	2.06	0.101	7.6	84.9	0.56	2195.2	0.066	1	0.6	0.007	0.36	0.9	3.1	0.13	0.03	6	b.d.	0.14	4.6
MMI03-6-2-2	6.82	0.001	b.d.	38.8	17.66	17	0.004	2	0.01	0.003	b.d.	b.d.	3.1	b.d.	0.06	b.d.	0.2	b.d.	0.1
MMI03-6-5	0.53	0.021	1.2	86.8	0.94	13.3	0.16	4	1.15	0.065	0.07	b.d.	6.6	0.02	0.63	12	0.2	0.04	5
MMI03-7-2	1.25	0.015	0.5	53.8	0.84	3.9	0.219	4	1.26	0.015	0.01	b.d.	4.4	b.d.	0.02	b.d.	b.d.	b.d.	3.7
MMI03-8-7	3.65	0.037	1.2	10.9	1.44	5.2	0.2	3	1.68	0.094	0.05	b.d.	1.6	b.d.	0.01	b.d.	b.d.	b.d.	6.9
MMI03-8-8	0.27	0.016	0.6	33.3	2.63	1.5	0.077	1	2.75	0.006	b.d.	b.d.	9	b.d.	0.11	22	20.9	0.09	10.1
Acme QC	0.64	0.088	2.4	42.2	0.97	25.4	0.172	1	1.3	0.05	0.11	0.2	5.9	0.04	1.47	b.d.	3.7	0.08	4.2
Silica blank	0.01	0.001	2.3	182.3	0.01	15.9	0.004	1	0.04	0.002	0.02	b.d.	0.1	b.d.	0.03	b.d.	b.d.	b.d.	0.1
BGR-1-001	0.82	0.012	b.d.	88.9	1.72	0.8	0.108	1	1.55	0.002	b.d.	b.d.	6.4	b.d.	7.04	35	7.1	0.22	4.9
Acme QC	0.7	0.092	11.2	183.1	0.64	134.6	0.087	17	1.99	0.032	0.13	4.8	3.4	0.98	0.03	170	4.5	0.82	6.5
STD GSB Till 99	0.32	0.101	13.6	237.4	2.43	227.8	0.085	1	2.64	0.004	0.04	b.d.	14.4	0.09	b.d.	292	0.3	0.25	8.2
Std. GSB Till 99	0.34	0.107	14.4	247.6	2.55	239.4	0.09	b.d.	2.77	0.005	0.04	b.d.	14.7	0.1	b.d.	305	0.4	0.25	8.6
	0.33	0.104	14	242.5	2.49	233.6	0.0875	1	2.705	0.0045	0.04	b.d.	14.55	0.095	b.d.	298.5	0.35	0.25	8.4
	0.0	0.0	0.6	7.2	0.1	8.2	0.0		0.1	0.0	0.0		0.2	0.0		9.2	0.1	0.0	0.3
	4.3	4.1	4.0	3.0	3.4	3.5	4.0		3.4	15.7	0.0		1.5	7.4		3.1	20.2	0.0	3.4

Note: see Table 2 for sample locations

TABLE 2. RESULTS OF INDUCED NEUTRON ACTIVATION ANALYSES (INAA)

Station Number	Easting	Northing	Element								
			Au	As	Ba	Ca	Co	Cr	Fe	Hf	Mo
			ppb	ppm	ppm	%	ppm	ppm	%	ppm	ppm
Detection Limit			2	0.5	50	1	1	5	0.02	1	1
LFE03-4-1	620020	6542337	1480	1.3	160	14	24	719	2.51	b.d.	b.d.
LFE03-17-4	624689	6541846	20	18	b.d.	7	34	196	13.5	1	b.d.
LFE-03-17-7	622472	6543267	4	15.9	b.d.	2	18	70	7.51	2	8
STD GSB Till 99			26	61.4	960	2	45	368	7.71	3	b.d.
MMI03-12-2	620487	6537407	20	11.9	85	b.d.	114	126	13.6	1	b.d.
MMI03-12-2-3	620487	6537407	b.d.	3.6	b.d.	b.d.	25	51	6.33	4	b.d.
MMI03-12-2-4	620487	6537407	26	2.5	b.d.	b.d.	88	190	11.1	b.d.	b.d.
MMI03-12-2-5	620487	6537407	5	28	b.d.	14	69	1800	4.18	b.d.	b.d.
MMI03-12-5	620463	6537537	b.d.	55.1	b.d.	4	63	2540	3.45	b.d.	b.d.
MMI03-2-11	620373	6544373	25	9.2	b.d.	b.d.	25	73	8.42	2	11
MMI03-25-14	623445	6542687	137	27.7	b.d.	1	26	35	7.08	2	b.d.
Std. GSB Till 99			36	60.4	930	b.d.	45	368	7.78	3	b.d.
MMI03-25-15b	623544	6542801	584	9.6	b.d.	b.d.	12	176	3	b.d.	21
MMI03-25-5	625137	6542383	b.d.	b.d.	b.d.	7	41	175	8.63	1	b.d.
MMI03-25-7	624802	6542092	43	6.7	b.d.	3	47	237	10.3	2	b.d.
MMI03-2-7	620314	6544344	76	31.5	b.d.	b.d.	302	98	12.4	2	18
MMI03-31-10a	618326	6545686	543	1.7	b.d.	14	75	480	5.06	b.d.	b.d.
MMI03-31-10b	618326	6545686	b.d.	2.8	430	12	78	525	6.61	b.d.	b.d.
MMI03-31-10c	618326	6545686	31	3	b.d.	14	71	1300	7.11	b.d.	b.d.
MMI03-31-10d	618326	6545686	b.d.	3.2	b.d.	11	125	1130	11.8	b.d.	b.d.
MMI03-31-12a	618432	6545725	48	13	b.d.	10	45	156	12.7	b.d.	b.d.
MMI03-31-12b	618432	6545725	b.d.	2.2	b.d.	7	44	1380	2.61	b.d.	b.d.
MMI03-31-12c	618432	6545725	29	3.4	b.d.	10	33	300	10.3	b.d.	b.d.
MMI03-5-19-1	621005	6541401	110	35.3	b.d.	5	33	196	6.73	b.d.	b.d.
MMI03-5-19-2	621005	6541401	39	5	b.d.	6	7	180	4.2	b.d.	b.d.
MMI03-5-6	620072	6542193	b.d.	3.7	24000	2	12	176	2.37	3	b.d.
MMI03-6-2-2	621633	6544264	b.d.	1.7	b.d.	7	6	49	2.06	b.d.	b.d.
MMI03-6-5	621933	6544290	b.d.	4.6	120	b.d.	8	151	2.53	2	b.d.
MMI03-7-2	619753	6544718	4	b.d.	b.d.	7	11	101	5.05	1	b.d.
MMI03-8-7	621232	6541095	5	b.d.	b.d.	9	29	29	7.22	2	b.d.
MMI03-8-8	621102	6540832	17	5.7	b.d.	2	59	69	16.6	b.d.	8
Silica blank			b.d.	1.8	b.d.	b.d.	1	359	0.33	b.d.	b.d.
BGR-1-001	621083	6541361	23	15.8	100	3	58	165	10.8	1	b.d.
QC											
STD GSB Till 99			26	61.4	960	2	45	368	7.71	3	b.d.
Std. GSB Till 99			36	60.4	930	b.d.	45	368	7.78	3	b.d.
Mean			31	60.9	945	2	45	368	7.75	3	b.d.
SD			7.07	0.71	21.21		0	0	0.05	0	
%RSD			22.8	1.16	2.245		0	0	0.64	0	
Silica blank			b.d.	1.8	b.d.	b.d.	1	359	0.33	b.d.	b.d.

TABLE 2. INAA RESULTS CONTINUED

Element	Na	Ni	Sb	Sc	Se	Th	Zn	La	Ce	Nd	Sm	Eu	Yb	Lu	Mass
Units	%	ppm	g												
Detection Limit	0.01	20	0.1	0.1	3	0.5	50	0.1	3	5	0.1	0.2	0.2	0.05	0.1
Station Number															
LFE03-4-1	0.26	b.d.	b.d.	26.4	b.d.	b.d.	b.d.	b.d.	b.d.	b.d.	0.2	b.d.	0.5	0.07	28.09
LFE03-17-4	0.03	b.d.	0.7	17.2	13	0.5	b.d.	3.4	8	b.d.	1.9	1.3	1.9	0.28	28.05
LFE-03-17-7	1.85	b.d.	0.7	18.1	b.d.	b.d.	638	2.3	5	7	1.9	0.7	3.1	0.46	28.56
STD GSB Till 99	1.75	244	13.8	27.6	b.d.	5.6	399	29.4	54	24	5.7	2.1	2.8	0.42	20.51
MMI03-12-2	0.34	b.d.	b.d.	11.4	21	b.d.	88	2.1	7	b.d.	1.2	0.6	1.3	0.22	31.46
MMI03-12-2-3	2.67	b.d.	b.d.	19.1	b.d.	b.d.	92	2.9	9	8	2.5	0.9	5.5	0.85	30.41
MMI03-12-2-4	0.26	b.d.	b.d.	7.5	40	b.d.	b.d.	1.4	b.d.	b.d.	0.8	0.4	1	0.15	29.06
MMI03-12-2-5	0.03	1050	1.9	6.4	b.d.	b.d.	55	b.d.	37.06						
MMI03-12-5	0.04	1070	8.1	2.5	b.d.	31.44									
MMI03-2-11	2.26	b.d.	0.3	17.5	4	0.4	2250	2.7	10	7	2.1	0.8	3.4	0.51	33.39
MMI03-25-14	2.48	b.d.	1.8	32.8	b.d.	b.d.	1550	2.2	11	7	2.1	0.8	3	0.48	30.38
Std. GSB Till 99	1.77	241	13.4	28.8	b.d.	5.8	431	30.1	54	23	5.8	2.2	3	0.46	23.58
MMI03-25-15b	1.08	b.d.	0.6	13	b.d.	b.d.	832	0.9	3	b.d.	0.7	0.4	1.1	0.16	25.41
MMI03-25-5	2.13	170	0.2	45.2	b.d.	0.4	155	1.7	5	b.d.	1.8	0.6	2.7	0.41	31.78
MMI03-25-7	2.47	b.d.	0.3	41.6	b.d.	b.d.	320	2.5	7	b.d.	2.5	1.2	3.2	0.47	31.6
MMI03-2-7	0.15	b.d.	2.1	16.7	53	b.d.	375	1.7	5	b.d.	1.4	0.2	2.2	0.35	29.25
MMI03-31-10a	0.08	130	b.d.	24.7	35	b.d.	178	0.6	3	b.d.	0.3	b.d.	0.4	0.06	31.71
MMI03-31-10b	0.46	74	b.d.	29.5	b.d.	b.d.	184	2.7	7	b.d.	1.1	0.6	0.9	0.14	31.2
MMI03-31-10c	0.11	290	0.8	37	17	b.d.	164	0.6	b.d.	b.d.	0.3	b.d.	0.6	0.09	36.49
MMI03-31-10d	0.08	327	0.2	27.2	26	b.d.	180	0.6	b.d.	b.d.	0.2	b.d.	b.d.	b.d.	29.51
MMI03-31-12a	0.05	b.d.	0.2	7.1	119	b.d.	76	0.6	b.d.	b.d.	0.2	0.7	b.d.	b.d.	30.1
MMI03-31-12b	0.03	741	0.3	3.6	b.d.	b.d.	b.d.	0.7	b.d.	b.d.	b.d.	b.d.	b.d.	b.d.	26.59
MMI03-31-12c	0.06	b.d.	b.d.	21.2	74	b.d.	111	0.9	3	b.d.	0.4	0.5	0.6	0.09	34.1
MMI03-5-19-1	0.02	b.d.	b.d.	11	7	b.d.	82	1.6	4	b.d.	1	0.5	1.5	0.23	29.45
MMI03-5-19-2	0.02	b.d.	b.d.	6.4	7	0.2	b.d.	0.9	b.d.	b.d.	0.5	0.5	0.7	0.11	33.32
MMI03-5-6	0.1	79	0.8	8.8	b.d.	1.6	78	18.9	16	13	3.4	0.8	2.3	0.36	30.43
MMI03-6-2-2	0.03	272	b.d.	3.5	b.d.	30.92									
MMI03-6-5	2.6	b.d.	0.8	11.9	b.d.	0.4	76	3.2	9	7	2.2	0.7	3.6	0.54	30.17
MMI03-7-2	0.73	109	b.d.	18.5	b.d.	b.d.	b.d.	2.1	5	b.d.	1.5	0.7	2.1	0.31	38.02
MMI03-8-7	2.54	b.d.	b.d.	34.8	b.d.	b.d.	b.d.	2.7	8	b.d.	2.2	0.8	3.3	0.5	30.24
MMI03-8-8	0.28	b.d.	b.d.	19.8	22	b.d.	113	4.6	11	b.d.	2.8	1.9	1.9	0.3	34.59
Silica blank	0.04	b.d.	0.1	0.5	b.d.	0.7	b.d.	4.5	7	b.d.	0.4	b.d.	b.d.	b.d.	28.88
BGR-1-001	0.16	196	b.d.	18.4	b.d.	b.d.	78	1.3	b.d.	b.d.	0.9	0.2	1.5	0.23	37.35
QC															
STD GSB Till 99	1.75	244	13.8	27.6	b.d.	5.6	399	29.4	54	24	5.7	2.1	2.8	0.42	20.51
Std. GSB Till 99	1.77	241	13.4	28.8	b.d.	5.8	431	30.1	54	23	5.8	2.2	3	0.46	23.58
Mean	1.76	243	13.6	28.2	b.d.	5.7	415	29.8	54	23.5	5.75	2.15	2.9	0.44	22.05
SD	0.01	2.12	0.28	0.85		0.14	22.6	0.49	0	0.71	0.07	0.07	0.14	0.028	2.171
%RSD	0.8	0.87	2.08	3.01		2.48	5.45	1.66	0	3.01	1.23	3.29	4.88	6.428	9.847
Silica blank	0.04	b.d.	0.1	0.5	b.d.	0.7	b.d.	4.5	7	b.d.	0.4	b.d.	b.d.	b.d.	28.88



Photo 2. Pillowed basalt flows are very well developed on “Sleeper Peak” immediately west of “Black Goat Peak”.

commonly, chert are locally preserved and present opportunities for age dating via microfossils, either conodonts or radiolaria. Interpillow or interflow hyaloclastite is recognizable in well preserved sections.

Agglomerate is exposed at the structural top of the pillowed section hosting the Joss’alun mineralization. The definition of “agglomerate” used herein is: a monomict volcanic breccia composed primarily of rounded clasts (bombs, not erosional).

On the eastern side of “Jos valley” the agglomerate grades into basalt breccia with a cherty ferruginous maroon matrix (Photo 3), which in turn, grades into ferruginous chert from which “Permian” radiolaria were extracted (Mihalynuk *et al.*, 2003b). The same stratigraphic relationship is seen on the west side of “Jos Peak”, suggesting a regionally correlatable succession (see also “Ferruginous chert” below).

Sections of basalt exposed within the NAK area probably span a range of ages, but no field criteria that permit



Photo 3. Volcanic breccia near the top of the mafic volcanic section commonly displays a maroon, cherty ash matrix. Locally this unit grades into ferruginous chert.



Photo 4. A typical exposure of ferruginous chert. Layer thickness of 1-5 centimetres and ruler straight beds are typical, but not displayed in all occurrences.

basalts of varying ages to be distinguished from one another have yet been recognized.

Geochemistry

We collected 5 samples of basalt from the belt of mafic volcanic rocks and probable correlatives within the Joss’alun belt and analyzed major, trace and rare earth elements in order to test the tectonic affinity of the parent magma(s). The data are given in Table 3 and plotted in Figure 6.

Figure 6A is a plot of alkalis versus silica with the alkali-subalkaline fields of Irvine and Baragar (1971); all samples are subalkaline. Figure 6B shows rock classification fields of Cox *et al.* (1979), all of the samples are basalt or basaltic andesite. Alkalis and silica can be mobile in metamorphosed rocks. However, the samples plot in corresponding fields based on their immobile elements composition (Fig. 6C, D; Winchester and Floyd, 1977), confirming the rock type assignment made on the basis of major oxides.

Discrimination of modern petrogenetic environments can be shown by plotting elemental abundances in basalts. Composition of ancient basalts can be compared with modern environments in order to resolve the tectonic environment in which they formed. The Th-Hf/3-Ta discrimination plot of Wood (1980) separates the geochemical fields of basalts generated at a destructive plate margin (arc) from

TABLE 3. RESULTS OF MAJOR OXIDE X-RAY FLUORESCENCE (XRF) ANALYSES

Field Number	Description	SiO ₂	TiO ₂	Al ₂ O ₃	Fe ₂ O ₃	MnO	MgO	CaO	Na ₂ O	K ₂ O	P ₂ O ₅	Xba	LOI	Total	Total	XRb	XSr	XBa	XNb	XZr	XHF
MM103-5-6	"Sleeper Peak" chert	79.26	0.15	2.43	3.35	0.47	1.07	3.00	0.23	0.75	0.15	2.56	3.04	96.46	26	76	25594	12	56	4	
MM103-3-2-1	Gabbro S of Joss alun, intrudes 3-2-2	46.95	0.27	7.09	8.18	0.14	18.79	13.35	0.25	0.01	0.01	0.01	4.28	99.33	5	20	24	3	17	<3	
MM103-3-2-2	Ultramafite intruded by 3-2-1	40.56	0.10	3.54	14.39	0.14	28.64	2.34	0.07	0.01	0.01	0.01	9.89	99.70	<3	<3	35	5	16	<3	
MM103-3-8*2	Jos - S pillow breccia atop clastics	49.15	1.05	14.38	10.05	0.18	6.42	9.10	2.18	1.15	0.10	0.01	5.92	99.69	12	128	64	<3	77	<3	
MM103-4-2	Hardluck Pks agglomerate	49.40	1.41	14.81	10.32	0.25	5.67	9.61	2.36	0.66	0.15	0.01	5.00	99.65	16	118	57	4	89	<3	
MM103-5-2*2	"Sleeper Pk." mafic fragmental	49.68	1.07	14.84	9.73	0.17	8.06	10.07	2.94	0.50	0.07	0.35	1.99	99.47	11	262	3502	4	63	3	
MM103-5-11-2	"Sleeper Pk." pillow basalt	50.09	1.50	15.25	11.75	0.15	5.94	10.06	3.40	0.20	0.18	0.01	1.29	99.82	6	134	67	6	97	4	
MM103-10-6-2	Pillow basalt NE Peridotite Pk	48.84	0.99	13.19	11.32	0.15	7.19	11.97	2.00	0.02	0.09	0.01	4.07	99.84	3	51	136	5	58	<3	
MM103-12-1	Yeth CK voics	48.22	0.43	13.35	8.02	0.14	10.47	9.85	1.97	2.01	0.10	0.01	4.59	99.16	23	173	145	<3	40	<3	
MM103-28-11	Dense basalt - McCallum Pk	52.11	1.47	17.05	10.17	0.14	3.50	4.48	5.59	1.90	0.38	0.15	2.53	99.47	43	721	1482	6	149	4	
MM103-25-5	Ald gabbro + cpy flecks - Unnamed Ck	47.97	1.49	14.68	11.39	0.14	7.63	9.55	2.64	0.03	0.07	0.01	4.05	99.65	6	45	37	<3	51	<3	
MM103-25-7	Basalt Ck between Peridotite and Hardluck	52.74	0.80	14.64	8.97	0.09	7.55	6.80	2.46	0.02	0.09	0.01	5.48	99.65	5	33	53	<3	58	<3	
MM103-27-2	Massive tuff. - Peninsula Mtn.	56.63	0.75	17.45	7.36	0.11	2.72	6.28	2.51	2.14	0.20	0.15	3.02	99.32	67	709	1499	4	128	3	
MM103-25-15a	Massive basalt flows - Unnamed Ck.	49.45	0.93	15.10	9.77	0.18	8.26	4.53	3.73	0.17	0.07	0.01	7.23	99.43	<3	72	83	<3	67	<3	
MM103-14-6	Foliated Granodiorite U-Pb S Hardluck	59.29	0.57	16.71	16.71	0.10	3.28	6.59	2.80	1.05	0.10	0.11	3.21	99.57	31	569	1066	3	91	3	
STD FER-3		53.52	0.01	0.07	44.43	0.07	1.00	0.83	0.01	0.01	0.09	0.01	-0.19	99.86	<3	29	20	<3	<3	<3	
Std. CANMET SY-4		49.81	0.28	20.65	6.21	0.10	0.52	8.03	7.03	1.62	0.12	0.03	4.80	99.20	53	1214	349	14	504	12	
Std. CANMET SY-4		49.81	0.28	20.65	6.21	0.10	0.52	8.03	7.03	1.62	0.12	0.03	4.80	99.20	53	1214	349	14	504	12	
SY-4 standard		49.90	0.29	20.69	6.21	0.11	0.54	8.05	7.10	1.66	0.13	0.03	4.56	99.27	55	1191	340	13	517	11	

TABLE 4. RESULTS OF TRACE ELEMENT ANALYSES (ICPMS)

Stn No	Y	Zr	Nb	Ba	La	Ce	Pr	Nd	Sm	Eu	Gd ⁶⁰	Tb	Dy	Ho	Er	Tm	Yb	Lu	Hf	Ta	Th	Nb _{Revis}
MM103-5-6	15.284	50.84	7.14	26304	18.33	14.64	4.309	17.88	4.00	1.13	3.72	0.588	3.54	0.687	2.01	0.304	2.09	0.35	0.99	0.19	1.81	3.54
MM103-3-2-1	7.023	5.42	3.75	31	0.15	0.58	0.143	1.04	0.56	0.25	0.97	0.193	1.44	0.297	0.87	0.125	0.82	0.12	0.23	0.02	0.01	0.23
MM103-3-2-2	1.916	1.59	3.99	17	0.05	0.18	0.043	0.28	0.15	0.09	0.25	0.048	0.36	0.078	0.24	0.038	0.25	0.04	0.07	0.02	0.01	0.49
MM103-3-8*2	22.402	87.39	6.09	82	3.02	8.65	1.452	7.97	2.71	0.98	3.61	0.652	4.35	0.857	2.56	0.373	2.34	0.36	2.24	0.16	0.19	1.93
MM103-4-2	29.220	104.40	5.36	60	3.70	9.87	1.877	10.68	3.59	1.30	5.18	0.870	5.68	1.198	3.51	0.491	3.10	0.44	2.70	0.11	0.15	1.40
MM103-5-2*2	18.212	69.49	7.27	4321	3.07	8.02	1.286	6.82	2.23	0.80	3.19	0.524	3.56	0.768	2.25	0.331	2.20	0.33	1.76	0.20	0.20	3.59
MM103-5-11*2	24.252	112.13	11.72	51	5.11	13.68	2.149	11.24	3.37	1.16	4.55	0.741	4.80	0.977	2.85	0.404	2.66	0.38	2.70	0.37	0.36	6.97
MM103-12-1	18.860	64.29	6.97	159	2.79	7.37	1.205	6.47	2.09	0.92	3.10	0.522	3.51	0.753	2.25	0.332	2.13	0.32	1.55	0.17	0.15	2.98
MM103-28-11	11.456	32.43	3.97	181	1.37	3.44	0.583	3.23	1.10	0.42	1.58	0.271	1.92	0.416	1.31	0.195	1.35	0.20	0.88	0.04	0.10	0.79
MM103-25-5	28.290	170.49	16.54	1836	22.03	43.83	6.105	27.24	6.08	1.73	6.33	0.909	5.42	1.082	3.03	0.430	2.80	0.41	3.77	0.52	4.03	9.58
MM103-25-7	17.076	56.81	3.82	15	1.28	4.34	0.798	4.53	1.73	0.60	2.68	0.490	3.38	0.701	2.14	0.312	2.12	0.32	1.55	0.07	0.12	1.64
MM103-25-7	17.211	59.72	3.02	55	2.05	5.94	1.023	5.71	1.97	0.80	2.82	0.497	3.35	0.686	2.06	0.303	2.00	0.30	1.64	0.06	0.14	0.86
MM103-27-2	18.201	140.77	9.26	1853	21.01	39.03	4.755	19.61	4.15	1.24	4.01	0.595	3.59	0.712	2.04	0.300	1.98	0.31	3.26	0.34	5.29	6.35
MM103-25-15a	34.174	157.59	11.02	1329	10.48	22.94	3.187	14.78	4.24	1.49	5.65	0.976	6.49	1.346	4.07	0.613	4.05	0.62	3.90	0.37	2.04	5.84
MM103-14-6	14.691	95.36	8.50	1295	9.15	18.13	2.263	10.04	2.35	0.80	2.66	0.455	2.95	0.592	1.83	0.274	1.87	0.29	2.33	0.37	1.92	5.84
Detect Limit	0.004	0.04	0.03	0.08	0.01	0.01	0.003	0.03	0.01	0.01	0.02	0.004	0.03	0.002	0.01	0.003	0.01	0.003	0.02	0.04	0.01	
Std. CANMET SY-4	103.94	697.51	21.49	402	56.12	114.44	14.14	57.57	12.51	1.99	14.65	2.742	19.67	4.392	14.64	2.342	15.58	2.11	12.31	0.81	1.15	16.36
CANMET Ref	119.00	517.00	13.00	340	58.00	122.00	15.00	57.00	12.70	2.00	14.00	2.600	18.20	4.300	14.20	2.300	14.80	2.10	10.60	0.90	1.40	13.00
percentDifference	13.507	29.73	49.21	17	3.30	6.40	5.924	1.00	1.51	0.45	4.51	5.316	7.74	2.117	3.06	1.810	5.15	0.43	14.95	10.53	19.69	22.89

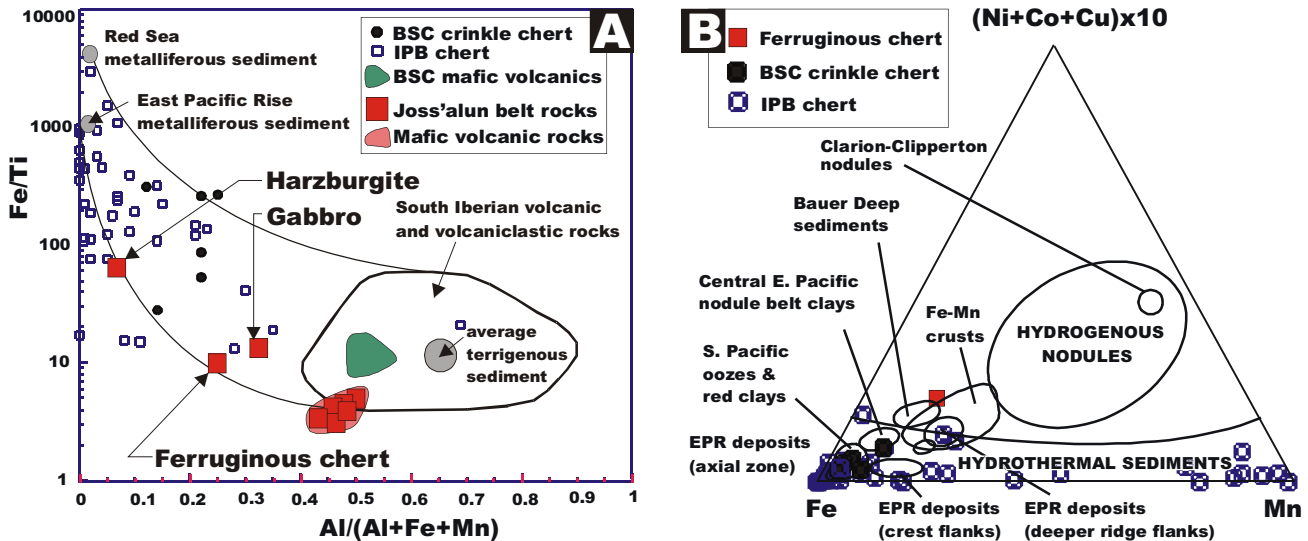
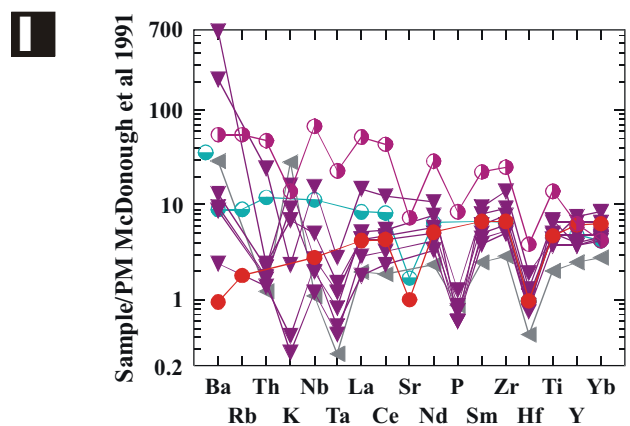
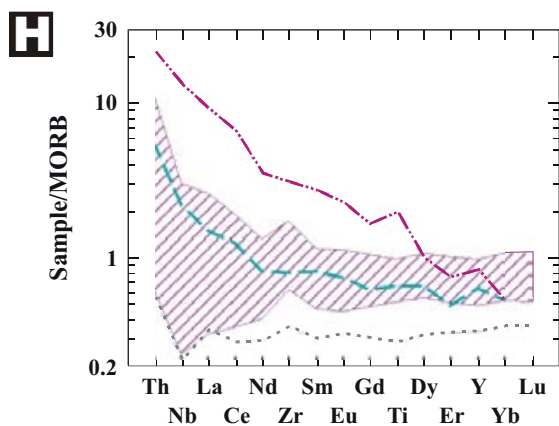
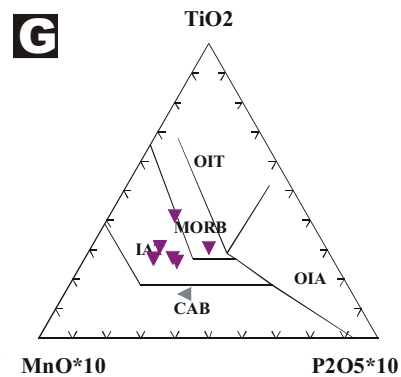
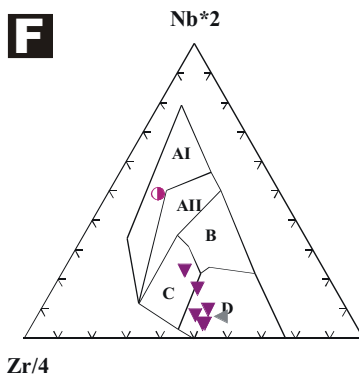
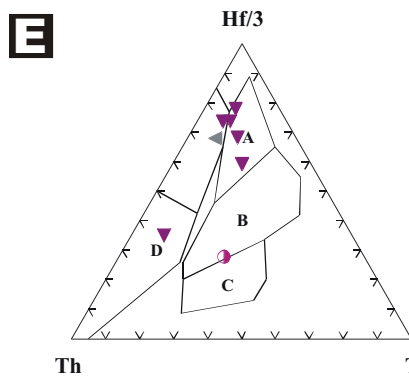
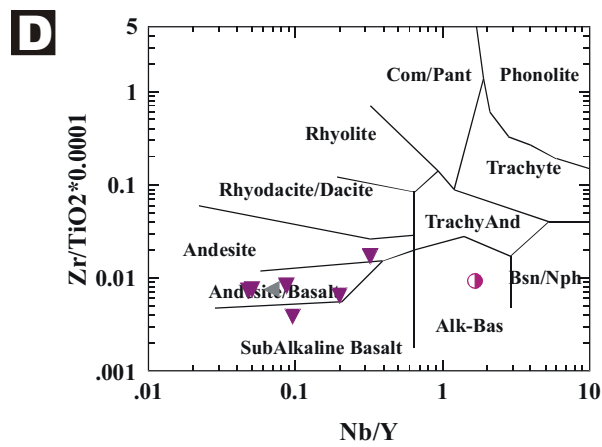
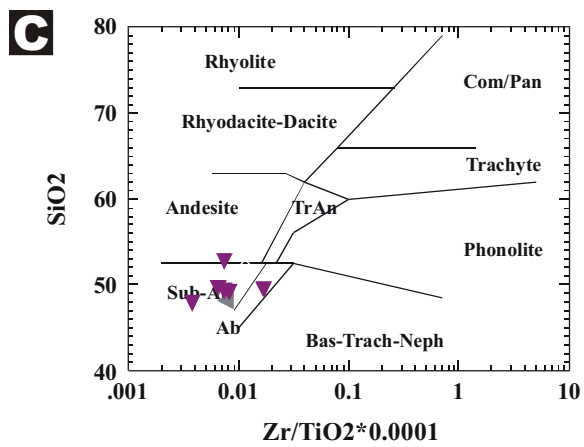
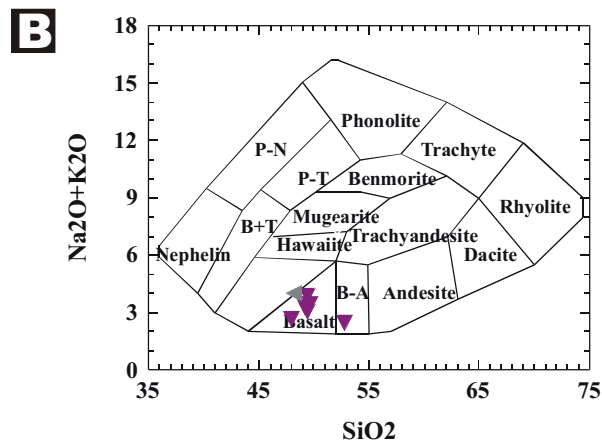
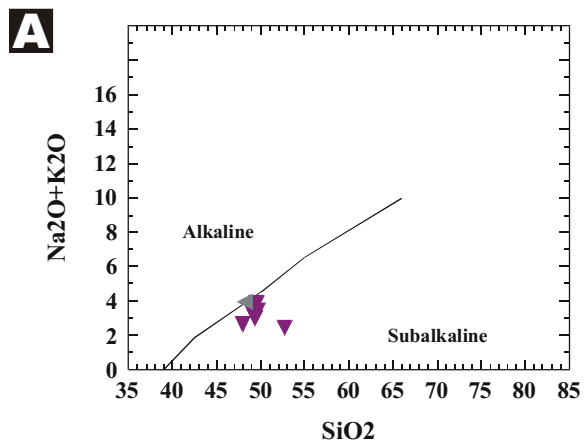


Figure 3. Chemical composition of ferruginous chert as compared on a plot of Fe/Ti versus Al/(Al+Fe+Mn) as a measure of the proportion of hydrothermal or terrigenous inputs (A), and on (B) the Ni+Co+Cu - Fe - Mn ternary diagram, to discriminate between hydrothermal and hydrogenous or biogenic sources (see Mihalynuk and Peter, 2001 for sources). Also compared are the composition of chert and volcanic rocks from the Big Salmon complex (Mihalynuk and Peter, 2001). Although the ferruginous chert unit is locally copper stained, elevated copper contents are common in oceanic settings and do not necessarily indicate a hydrothermal source. Ferruginous chert chemical composition plots within between the fields of hydrothermal sediment and terrigenous sediment (A) and with deep sea sediments and Fe-Mn crusts (B).

TABLE 5. RESULTS OF RADIOLARIAN PROCESSING AND IDENTIFICATION IN 2003

Samples	Location UTM zn8 E/N	Lithology	Radiolarian Occurrence	Preser- vation	Content and radiolarian taxa	Age
MMI03-3-10	618779 6544207	red chert	+	poor	sponge spicules, recrystallized spumellarians, silica fragments	indeterminate
MMI03-5-3	620190 6542388	laminated grey/black siliceous argillite	?	/	silica fragments, one conodont specimen sent to M.J. Orchard, Geological Survey of Canada, Vancouver	see M.J. Orchard
MMI03-5-5	620090 6542240	grey siliceous argillite	+	poor	abundant recrystallized flattened radiolarians. Large triradiate <i>Latentifistulidae</i>	Carboniferous-Permian
MMI03-5-6	620070 6542195	red chert	+	very poor	recrystallized silica fragments, red clays	indeterminate
MMI03-5-12	620346 6541664	red chert	+	poor	sponge spicules, silica fragments, large <i>Latentifistulidae</i> , ? <i>Quinqueremis</i> sp.	Carboniferous-Permian
MMI03-7-3	619800 6544550	grey-brown siliceous argillite	+	poor	silica fragments and aggregates, rare spumellarians	indeterminate
MMI03-10-5-2	632156 6541448	grey chert	+	moderate	<i>Haploaxon</i> sp., <i>Latentifistula</i> sp., <i>Pseudoalbaillella sakmarensis</i> , <i>Quinqueremis</i> sp.	Early Permian, late Asselian-Sakmarian
MMI03-10-8	632946 6540788	black chert	+	moderate	<i>Entactinia</i> sp., <i>Latentifistula</i> sp., <i>Pseudoalbaillella sakmarensis</i> , <i>Quinqueremis</i> sp., abundant quartz crystals	Early Permian; late Asselian-Sakmarian
MMI03-11-2	629051 6541445	grey chert	+	good	<i>Canesium lentum</i> , <i>Capnodoce</i> sp., <i>Capnuchosphaera schenki</i> , <i>Sarla</i> sp., <i>Saitoum</i> sp., <i>Triassocampe</i> sp.	Late Triassic, latest Carnian-early Norian
MMI03-12-11	620588 6540268	grey chert	+	poor	quartz crystals, sphaeromorphs, probable spumellarians	indeterminate
MMI03-14-9c	619500 6540030	grey chert	+	poor	silica fragments, sponge spicules, quartz and pyrite crystals, ? <i>Oertlispongos</i> , <i>Triassocampe</i> sp., recrystallized spumellarians and nasselarians	Middle or Late Triassic

Chemical procedure: HF 7%, 3 series of 24 hours for each sample



-  Joss'alun volcanics
-  Yeth Creek formation
-  Mid Ocean Ridge Basalt
-  Enriched MORB
-  Ocean Island Basalt

Figure 4. Geochemical plots show that the volcanic rocks in the study are subalkaline basalt based upon major oxide analyses (A, method of Irvine and Baragar, 1971; B, method of Cox, 1979) and trace elements (C, D; based upon method of Winchester and Floyd, 1977). Consistency between A, B and C, D provides a test for the reliability of the trace element analyses. Petrogenetic environment is shown in discrimination plots E, F, G (method of Wood, 1980; Meschede, 1986; and Mullen, 1983). Samples fall within or straddle the boundary between destructive plate margin (field D) and normal MORB (field B, field AI is within-plate basalt/EMORB field) on the Th-Ta-Hf/3 plot (Figure E). Figure F likewise shows that data straddle the boundary between volcanic arc basalt (fields C-D) and NMORB (field D); within plate alkaline basalts fall within field AI. Figure G similarly shows that samples straddle the fields between MORB and island arc tholeiite (IAT); CAB is the field of calc-alkaline basalt.



Photo 5. Copper staining on argillaceous bedding planes at the interbedded contact between marley ferruginous chert and limestone.



Photo 6. Chert layers in recrystallized limestone are typical of the best developed limestone sections.



Photo 7. A typical exposure of well-bedded, grey ribbon chert.

those formed in other environments. Basalts from the Joss'alun belt as well as the Yeth Creek formation fall within or straddle the boundary between the volcanic arc field (VAB) and normal Mid-Ocean Ridge Basalt (N-MORB). Plotting Th-Hf/3-Nb/16 (not shown) yields nearly identical results and confirms the consistency of Nb and Ta analyses. In a plot of Zr/4-Y-Nb/2 after the method of Meschede (1986) the Joss'alun belt samples fall within the volcanic arc basalt and N-MORB fields (D); Yeth Creek formation falls in field D. The Ocean Island Basalt (OIB) and N-MORB standards fall into the expected within-plate (AI) and N-MORB (D) fields. Figure 6G shows the TiO_2 -MnO- P_2O_5 plot after the method of Mullen (1983). On this plot, Joss'alun belt samples fall within the Island Arc Tholeiite and MORB fields while the Yeth Creek formation sample falls within the Calc-Alkaline Basalt field.

On the variation diagrams (Fig. 6H, I) the sample compositions are plotted normalized to MORB and Primitive mantle respectively. Figure 6H shows that the file of Joss'alun belt samples overlaps MORB and E-MORB, but are more depleted (except for heavy REEs) than OIB. They also display Nb depletion, as does the Yeth Creek formation sample, which is more depleted overall than MORB. Figure 6I shows depletion of Ta, P and Hf when compared with primitive mantle composition. K is depleted in two Joss'alun belt samples, whereas the others show enrichment of all Large Ion Lithophile (LIL) elements (Ba, Rb, K). Depletion of Nb and Ti, is typical of arc magmatism. Elevated LILs are consistent with magma generation above a subducted slab, and elevated values of both Th and Hf may indicate crustal contamination.

This small geochemical data set is most consistent with generation of Joss'alun belt magmas within an environment which has geochemical characteristics of both arc and within-plate sources. Modern environments which display similar chemical heterogeneity include back arc settings. Geochemical characteristics displayed by the Yeth Creek formation sample are most consistent with a volcanic arc setting.

FERRUGINOUS CHERT

Bright maroon ferruginous chert is a persistent unit that occurs structurally above the basalt unit at several localities in the NAK area. It has an estimated stratigraphic thickness of 5 m, although it can attain structural thicknesses in excess of 20m. Ruler straight 2-4 cm thick beds are characteristic (Photo 4), but locally beds can be bulbous and 10+ cm thick. Argillaceous interlayers are less than 1 cm. Radiolaria are common (Photo 9). At one locality the unit is malachite-stained (Photo 5). Trace element geochemical analysis of the chert unit shows that it is elevated in Cu and Ba (Tables 1 and 2), but such values fall within the range of normal hemipelagite (Figure 3).

Away from the basalt, ferruginous chert passes into limestone via increasing numbers of medium to thin limestone beds across a section typically two metres or less in thickness. Ferruginous chert above the basalt may correlate with a similar unit within the Hardluck clastic unit (see below).

Age of ferruginous chert

At one locality, the ferruginous chert yields Permian radiolaria (Mihalynuk *et al.*, 2003b) and one conodont element recovered from a different locality is of Carboniferous to Early Permian age (M. Orchard, written communication, 2003). A common age range of Early Permian is the assumed age of the ferruginous chert unit. This age assignment relies upon the assumption that the ferruginous chert at both localities is correlative and coeval.

LIMESTONE

Recrystallized, foliated limestone forms a layer with a maximum average structural thicknesses of 20 m, although the unit is commonly only a few metres thick or represented by brown or grey marley layers at the “upper” contact of the ferruginous chert unit (Photo 5). It is light grey to tan (dolomitic?)-weathering, with beds 2-10cm+ thick. It is commonly interbedded with dark grey, irregular chert beds of equal thickness (Photo 6). Some chert beds are laminated. Best exposures are on the western side of upper “Jos valley”.

WELL-LAYERED, GREY CHERT

Chert layers abruptly increase in abundance above the limestone forming a section of light to dark grey ribbon chert. Some sections of this unit are much more than 10m thick. Chert beds are normally 2-10 cm thick, continuous, and are interlayered with argillaceous beds less than 1.5 cm thick (Photo 7). Ribbons locally give way to massive laminated chert in beds a metre or more in thickness. Laminations are 1-3 mm thick and are thought to signal chert formed from a siliceous argillite progenitor. Grey chert grades rapidly into rusty chert; although the contact is commonly modified by faulting.



Photo 8. Granitoid clasts in ferruginous chert demonstrates consanguinity between Hardluck formation and an episode of ferruginous chert deposition.

RUSTY CHERT

Eye-catching, rusty-weathering ribbon chert has a thickness that varies dramatically from place to place, probably because it is the locus of thrust faults and subject to structural thickening and thinning. Maximum structural thickness is more than 100m. In some sections it has been cut out entirely or is present as fault-bounded lozenges a few metres thick. Ribbed chert beds are 2-10 cm thick and tan coloured on fresh surfaces. Locally it is rubbly weathering and a fresh surface can be difficult to obtain. Argillite interbeds are typically 0.5 cm thick, up to 2 cm thick, pyritic, bleached and stained by yellow jarositic clays. At several localities west of upper “Jos Creek”, the unit structurally overlies basalt.

MÉLANGE

Mélange is a structural unit that is interpreted to be younger than most other units within the NAK area. Much

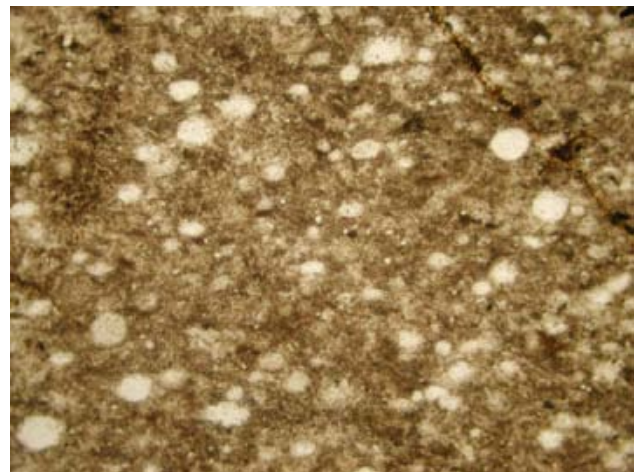


Photo 9. Photomicrograph shows recrystallized radiolaria. These are not well enough preserved to permit an age assignment.

of the low-lying areas south and east of the NAK property are underlain by serpentinite mélangé. Serpentine may comprise more than 50% of areas several square kilometres in size; knockers up to a square kilometre or more are enveloped by the serpentinite. Most common knocker types are serpentinitized harzburgite, chert and mafic volcanic knockers, but almost any lithology can be found within this tectonic unit, including ferruginous chert and volcanic sandstone. Knockers of coarse conglomerate belonging to the Hardluck formation (see below) are not observed, although volcanic sandstone knockers which are lithologically similar to restricted units within the Hardluck formation do occur.

A structural panel of blue-grey Middle to Late Triassic radiolarian-bearing cherty volcanic siltstone occurs between the mélangé and the overlying succession that includes Permian chert (Location A, Figure 2). Blocks of similar cherty volcanic siltstone occur within the mélangé unit. If the blocks are correctly correlated, the age of the mélangé must extend at least into the Middle Triassic.

HARDLUCK FORMATION

Polymictic, granitoid boulder conglomerate, and quartz-rich arkosic lithic sandstone characterize a succession of very immature clastic rocks that we informally refer to as the Hardluck formation. It is widespread on the northern flanks of Hardluck Peaks. One of the most conspicuous types of clast is porphyritic granitoid boulders. These locally dominate a mix of other clasts derived from lithologies within the Cache Creek complex: chert, mafic volcanics, limestone, and ultramafite (in order of decreasing abundance). Soft sediment deformation, olistostromal deposits and basin cannibalization, result in drastic facies changes, variability of bedding, flips in facing directions and innumerable intraformational unconformities. A number of the units formed as fault scarp talus and submarine landslide debris, which contain blocks up to the size of small cabins.

Previous observations led to the suggestion that in all areas Hardluck clastic rocks rest on mafic volcanoclastic strata (Mihalynuk *et al.*, 2003a). However, observations made during the 2003 field season show that volcanic flow breccia locally rests on an angular unconformity above the clastic unit and that granitoid conglomerate lenses are intercalated with maroon chert (Photo 8) that may correlate with the ferruginous chert unit. At two localities, Hardluck conglomerate rests on (or structurally overlies) marly ferruginous chert and is intercalated with mafic tuff. The unit could be diachronous, as old as Early Permian (age of ferruginous chert), and at least as young as Earliest Triassic detrital zircons that it contains (Mihalynuk *et al.*, 2003b). Middle Triassic radiolaria have been extracted from in a cabin-sized block near the base of the unit (Location B, Figure 2), but it seems unlikely that a small, tectonically active basin could have remained active and received very coarse detritus over such a long period of time. A thrust fault mapped between the Hardluck formation and the well-exposed stratigraphy on "Sleeper Peak" is interpreted to also

juxtapose the Middle Triassic chert unit with older rocks of the structurally overlying Hardluck formation.

VOLCANIC SILTSTONE/CHERT

Structural domains of blue-grey volcanic siltstone and chert are mapped across areas of less than ~ 1 km². Very fine laminations and delicate, well-preserved volcanoclastic textures characterize the unit. Bed thickness ranges from millimeters to decimeters and compositions range from light green tuff, to white, grey or black thick bedded, to thinly ribboned chert. Silty argillaceous beds are a conspicuous blue-grey colour. Where measured, folds within the unit have variable orientations, not concordant with folds of similar scale in adjacent panels. Thus, the unit appears to exist in isolated structural panels between the mélangé and other coherent units. However, at one locality (Locality C on Figure 2), the unit may grade into the Hardluck clastic unit. Radiolaria extracted from this unit indicate a Middle or Late Triassic age (MMI03-14-9c, Table 5).

Nak Structure

Rocks within the NAK area have been subjected to a protracted series of deformational events that have affected different parts of the area to varying degrees. A preliminary structural history is presented here:

- an early fold and thrust event juxtaposed panels of layered units (Photo 10). A common décollement surface appears to be the rusty chert unit (Figure 2, Location C).
- an episode of extensional faulting led to formation of basins receiving Hardluck clastic detritus. Small-scale extensional structures within the Hardluck unit are common (Photo 11) and likely mimic basin-scale structures (a possible example is at Location D, Figure 2). Extensional basin formation was probably coextensive with the duration of Hardluck clastic deposition. Minor volcanism appears coeval with extension as breccia units overly local angular unconformities within the Hardluck clastic unit. Extension may have affected the entire crust, leading to exposure of the mantle rocks and their serpentinitization. Within the main harzburgite body, there is no deformational fabric that post-dates emplacement of pyroxenite dikelets in a probable mantle setting, indicating that strain was highly partitioned, with the harzburgite acting as a rigid body during emplacement and subsequent deformational episodes. Strain was most likely focused at serpentinitized fault boundaries.
- A second episode of contractional deformation produced open to isoclinal, mainly upright folds with variable orientations, and thrust faults that cut previously folded and thrust faulted units (e.g. Figure 2, Locations E, F; Figure 12). The old detachment faults were probably reactivated as a major décollement surface. Motion along this fault produced serpentinite mélangé or increased the volume of mélangé units adjacent serpentinitized ultramafite. Above these units, many of the structural panels were translated. The large size of some knockers argues against entrainment of knockers as "xenoliths" during serpentine diapirism or



Photo 10. Layering in mafic tuffaceous rocks is cut by a thrust fault that juxtaposes them with recrystallized limestone below. Subsequent deformation has folded the thrust.

subduction zone backflow, at least when compared to modern analogues. Volcanic sandstone within mélangé constrains the age of mélangé formation to postdate the coarse clastic unit (if such a correlation is correct).

- A third, mainly south-verging fold and thrust event deformed earlier thrust faults; and produced a third generation of thrust faults. Deformation outlasting motion on the major décollement produced kilometre-scale, flame-like infolds of serpentinite mélangé as offshoots of the main ultramafite belt (Fig. 2, locations G and H), or infolding with other units on a finer scale (Fig. 2, location I). Folds related to this event exert a fundamental control on the present day distribution of rock types within the study area as well as the Early to Middle Jurassic Laberge Group strata to the southwest. This phase of deformation is probably related to a short-lived event between 174 and 172 Ma (Mihalynuk et al., 2004) related to emplacement of the Cache Creek terrane.

- Motion along the Nahlin fault may be kinematically linked to late strike-slip and dip-slip faults that cut third-phase folds within the NAK area (e.g. Figure 2, location J, K) and local injection of serpentinite between crustal blocks.

- The Nakina River stock cuts all major structures and thermally metamorphoses all deformed units. It is dated as 174.5 ± 1.7 Ma (Villeneuve and Mihalynuk, unpublished).

- Relatively minor high angle faulting and reactivation of earlier-formed faults resulted in concentration of brittle deformation in a ~1m wide zone near the eastern margin of the Nakina stock. Dehydration of serpentinite during and following emplacement of the stock may have resulted in dilation and minor block faulting.

- Neogene slump failure of serpentinite mélangé has caused numerous landslides within the belt. Neogene extensional cracks riddle the harzburgite at Hardluck Peaks. The set of open fractures that are conspicuous from the air (Photo 12). Future failure of this unit could be catastrophic, and may result in blockage of the Nakina River.

Mineralization

Mineralization at the Joss'alun was evaluated through further surface mapping, trenching and drilling by Imperial Metals Corporation. New mineralization was discovered as part of the regional mapping in the Joss'alun belt both northwest and southeast of the Joss'alun prospect. Including these new showings, the present along-strike extent of mineral showings is now approximately 7.5 km. Mineralization was also found south of the Joss'alun, at the head of "Jos Creek", and farther south still, along the Nahlin Fault, on the south flank of Hardluck Peaks. New showings are called the "Joeboy", "NIC", "Leefer", and "Yeth" respectively (Figure 2).

JOSS'ALUN

Further work on the Joss'alun mineralization has extended the known limits of the mineralized zone at surface to at least 40 metres beyond its previously reported north-western extent. In places the mineralization appears to be brecciated and is perhaps controlled by faulting (Photo 13). In other places, evidence points to a syngenetic origin for the most substantial sulphide lenses. Evidence for syngeneses includes:



Photo 11. Evidence for extension within the Hardluck formation is widespread. An example of small-scale extensional faults is well displayed here where outlined by quartz veining.

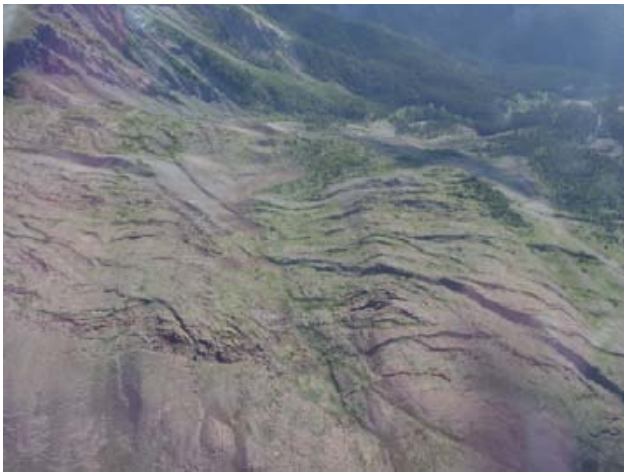


Photo 12. Aerial photograph of Neogene tension cracks within the main harzburgite body north of Hardluck Peaks. The rock mass is moving down slope, towards the Nakina River.

- near the main sulphide lenses: banding in some of the fine-grained sulphides and interlamination with silica-rich layers of possible exhalative origin (Photo 14).

- light grey, quartz-phyric felsic clasts are found in the hyaloclastite horizon above the main sulphide lens. They are an indicator synchronous felsic volcanism. Their presence raises the possibility of Kuroko-style mineral occurrences. A sample of the unit was collected for U-Pb geochronology.

- chalcopyrite mineralization is clearly focused along some of the pillow margins, suggesting extrusion of the flows onto unconsolidated sulphide mud.

A diamond drilling program was conducted on the NAK Property by Imperial to test the Joss'alun and the Jennusty showing (~2 km to the northwest). Nine holes, totalling 1,511 metres were completed with seven testing the Joss'alun, five of which intersected widespread copper mineralization. The mode of occurrence of copper is stringers, disseminations and pods of chalcopyrite with minor associated chalcocite.

The unit hosting the copper mineralization is comprised of a series of basaltic flows and breccias which have been faulted and folded, resulting of both the stacking and extension of the volcanic package. The brecciated units are heterolithic and probably reworked, containing sub-rounded clasts with evidence for multiple episodes of brecciation. Alteration associated with copper mineralization is most commonly quartz +/- calcite with accessory epidote and chlorite. Alteration intensity ranges from complete invasion and replacement of the host rock to flooding of the matrix or fractures, or simply amygdular infilling. Chalcopyrite can also occur in the pillow basalts as pillow rinds, hairline fracture filling or disseminations without quartz/carbonate alteration.

The best intercepts of the drill program include hole NAK-03-05, drilled beneath the main Joss'alun showing, with 17.75 metres of 0.94% copper; and hole NAK-03-07 with 53.45 metres of 0.34% copper. The most easterly drill hole, intersected mainly tuffaceous units intermixed with

basaltic flows, believed to be in the hangingwall of the pillow basalts that host the copper mineralization. Drilling results confirm that the volcanic stratigraphy on the NAK Property hosts considerable copper mineralization over a large area and is open along strike in both directions and to depth.

Cumulative evidence points to a mafic dominated VMS setting for the concordant massive sulphide lenses at the Joss'alun prospect. However, remobilized sulphide textures or discordant veins are clearly displayed, particularly in diamond drill core.

LEEFER BOULDER SHOWING (NEW)

Near the head of "Jos Creek", on the east side of the valley, is moraine that contains blocks of mafic volcanic and fine-grained diorite cut by quartz-epidote-chalcopyrite veins that occur in sheeted sets. We have named the showing the "Leefer". Boulders which are most intensely mineralized contain approximately 10% chalcopyrite as blebs within a 20cm thick quartz-epidote (+prehnite?) vein (Table 1, Sample MMI03-5-19-1, 1.5% Cu, >6 g/t Ag).

Attempts to trace this mineralization back to source were unsuccessful. Gossanous zones in the col east of "Black Goat Peak" contain 2-15% pyrite over widths of nearly a metre and several metres long, but they lack chalcopyrite. Centimetre-thick epidote-quartz veins containing chalcopyrite and pyrite were found south of "Black Goat Peak", but chalcopyrite was not nearly as abundant as in the moraine blocks. Considering the current physiography, the boulders seem most probably to have been derived from the north side of the mountain where no mineralization could be found. Considering the possible effects of continental glaciation, an alternative down-valley source is possible.

At least one period of glaciation with southward (up-valley) ice movement is suggested by extensive harzburgite boulders in the moraine that extends up the valley from the main harzburgite exposures. Up-valley transport of harzburgite erratics probably occurred during continental glaciation. Mineralized blocks may have likewise been car-



Photo 13. Fault planes above and below a rusty lens of pyrite-chalcopyrite at the Joss'alun occurrence. In contrast, many of the sulphide lenses do not show evidence of structural control.

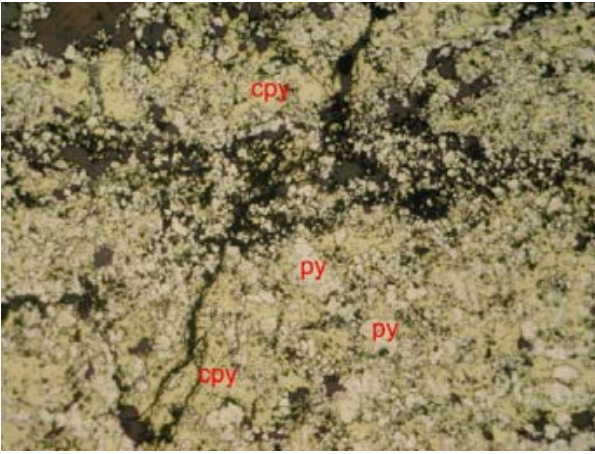


Photo 14. Banding within a sulphide lens near the discovery outcrops at the Joss'alun occurrence hints at a syngenetic origin. Photomicrograph width represents ~4mm, cpy = yellow chalcopyrite, py = white pyrite.

ried southward by continental glacier ice and then redistributed by valley glaciers at the close of the Quaternary. Similar mineralization is found in place at the NIC occurrence to the south (see below).

“MOHO SADDLE” VEINS (NEW)

Two families of veins crop out below the saddle in which the contact between harzburgite and gabbro is exposed, here called “Moho Saddle” (locality L, Figure 2). Most conspicuous is a white-weathering outcrop easily visible from across the valley. It comprises a 2 m thick vein composed of a tan to flesh-coloured, polygenetic, magnesite breccia. Much of the magnesite is probably finely intergrown with quartz, because it is unusually hard. At this locality, the vein is cut by several generations of chalcidonic and cocks-comb quartz veins, typically oriented at a high angle to the magnesite vein contact. Veins of similar character, but with thicknesses of 20 cm or less, crop out in the creek valley to the immediate north. Geochemical analyses (Tables 1 and 2) confirm visual indications of a barren vein system. Magnesite probably formed as a result of CO₂-charged fluid interacting with the adjacent Mg-rich rocks.

Immediately north of the main creek draw the mountain slope is littered with angular blocks of orange-brown-weathering gabbro cut by veins of milky white prehnite-quartz with knots of chalcopyrite up to 1.5cm in diameter. Although the blocks are not in place, they are believed to be of local derivation as they are mainly gabbro comprised of coarse orthopyroxene (4-15 mm; 30%) and altered plagioclase. Rocks cropping out in the immediate area are predominantly of this lithology. Analysis of the sample containing chalcopyrite yielded 0.15% Cu (LFE03-4-1, Table 1) and nearly 1.5 g/t Au (Table 2).

YETH OCCURRENCE (NEW)

A steep draw is cut into intensely fractured rocks along the Nahlin fault, which juxtaposes a package of unnamed

volcanic strata here called the “Yeth Creek formation” with serpentinized harzburgite. Between elevations of 900 m and 1100 m the draw is a shallow slot canyon less than 3 m wide with a bedrock floor and unstable bedrock walls capped by up to ~80 m of glacial till. This is the only location known to the authors where it is possible to walk on exposures of the Nahlin fault (locality M, Figure 2).

Sub-vertical listwanite alteration zones along the Nahlin fault trend 125°. Cinnabar occurs as coatings on fracture surfaces near the margins of listwanite alteration zones. At the lower end of the canyon, the Yeth Creek formation contains tabular, rusty, pyrite-flooded zones up to 2 m thick. The zones are approximately vertical and trend 090°.

A ~10m by 10 m exposed area contains pyrite chalcopyrite pods 1 to 15 cm thick and up to 1 m long spaced ~2m apart. This is the principle exposure of the Yeth occurrence. Two sets of irregular sulphide layers are apparent with orientations clustering around 145/50° and 075/70°. Three grab samples of sulphide plus country rock were carefully collected from the unstable canyon walls. A sample of a 10 cm thick ~2m long vein yielded 0.88% Cu and 0.6 g/t Ag (MMI03-12-2-1, Table 1). A ~3 cm thick chalcopyrite-rich layer within one of the ~2 m wide pyritiferous zones yielded 3.3% Cu and 1.9g/t Ag (MMI03-12-2-4). Further exploration of Yeth Creek formation may be warranted, however, these rocks tend to form steep and dangerously unstable exposures.

JOEBOY SULPHIDE OCCURRENCE (NEW)

Bright red ferruginous cherty ash and intercalated green volcanic lapilli tuff and breccia is well exposed along the steep walls of a 2 - 4 m wide, unnamed, south-flowing creek between Hardluck peaks and Peridotite Peak. Unlike ferruginous chert elsewhere, distinct bedding is not displayed, but the unit's structural thickness is estimated as tens of metres. Numerous rusty zones occur at the contact with the adjacent mafic volcanic unit. Within one rusty zone, above the exposed creek section, angular blocks of strongly pyritic mafic volcanic rock were recovered from amongst moss-covered tree roots (Figure 2, Location N). Pyrite comprises up to ~20% of decimeter-sized blocks, with accessory chalcopyrite. Analysis of one such block yielded 0.22% Cu (LFE03-17-4; Table 1). Mineralization at the Joeboy makes it notable, but more important is the existence of chalcopyrite-pyrite mineralization 5 km along strike from the pyrite-chalcopyrite lenses at the Joss'alun occurrence.

NIC COPPER OCCURRENCE (NEW)

Serpentinized and extensively faulted gabbro is exposed immediately south of the main harzburgite body, west of the ridge that extends north from “Jos Peak”. Quartz - carbonate - chalcocite - bornite and quartz-epidote-chalcopyrite-pyrite +/- bornite veins within the gabbro contain up to 3 cm thicknesses of chalcocite (in outcrop, Photo 15A) and 10 cm thicknesses of chalcopyrite (in talus

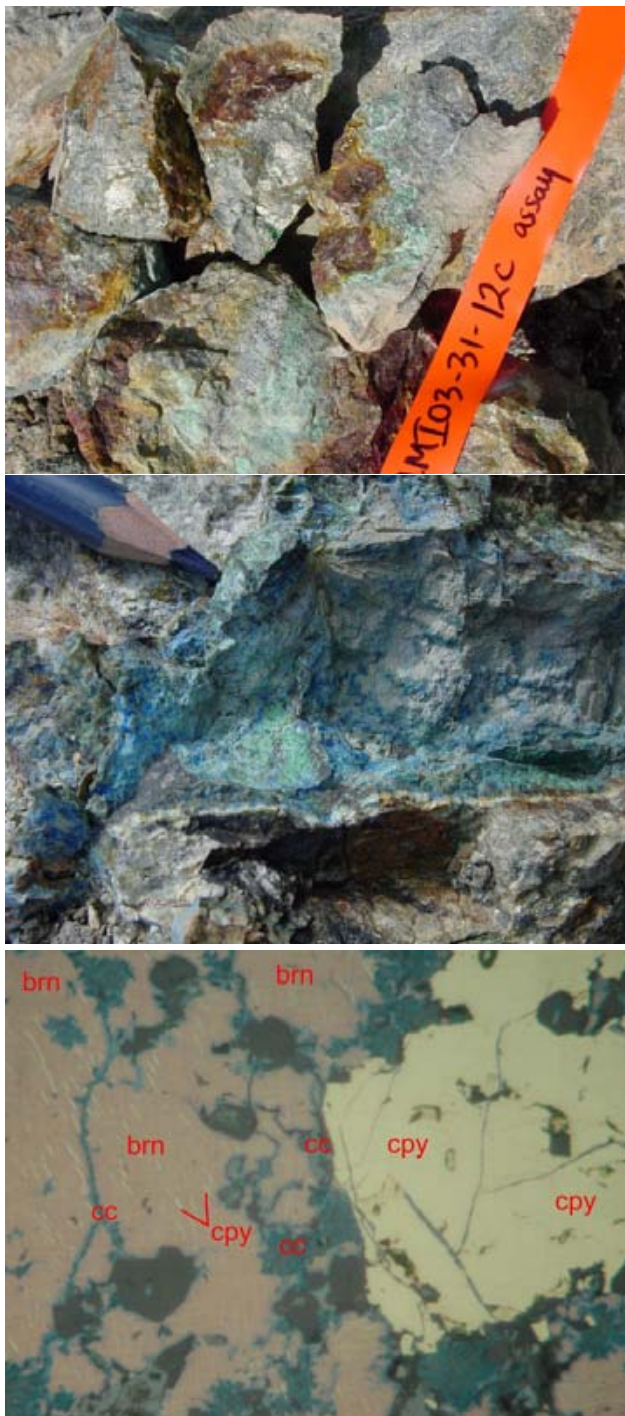


Photo 15. Mineralization at the NIC showing occurs mainly as (A, top) chalcopyrite veins up to 5 cm thick (Table 1, sample MMI03-31-10b) and (B) bornite-chalcocite/digenite veins up to 2 cm thick. Photomicrograph of chalcocite/digenite invading fracture and gangue boundaries in chalcopyrite and bornite. Also note exsolution lamellae of chalcopyrite in bornite (C, bottom). cpy = chalcopyrite, cc = chalcocite/digenite, brn = bornite (purple). Photomicrograph width represents ~ 0.1mm.

blocks, Photo 15B). Chalcopyrite-rich veins trend due west and dip steeply north (265/80). Analysis of mineralized grab samples yield values of ~3.4% Cu and 3.4 g/t Ag (2 cm

chalcocite vein in outcrop, MMI03-31-10a, Table 1); 1% Cu (chalcopyrite-bornite pods in outcrop, MMI03-31-10b); 3.8 % Cu and 1.8 g/t Ag (chalcopyrite vein, MMI03-31-10c); 4.6% Cu (2 cm chalcopyrite-bornite vein in outcrop, MMI03-31-10d); 7.3% and 6.0% Cu with 4.2 and 3 g/t Ag (MMI03-31-12a, c; quartz-epidote-chalcopyrite-pyrite veins, 6 cm thick, in talus blocks). Similar quartz-epidote-chalcopyrite-pyrite veins resemble those found in moraine at the Leefer showing, about 3 km south, up “Jos Creek” valley.

Mineralization at the NIC occurrence is significant because it extends the known limits of sulphide mineralization within the Joss’alun belt an additional ~2.5 km north-west of the Joss’alun prospect.

Geological History

Oldest strata within the northern Cache Creek terrane are Early Mississippian chert (Monger, 1975) and Pennsylvanian carbonate (Mihalynuk, *et al.*, 2003a) interbedded with volcanic strata of ocean island parentage (English, *et al.*, 2002). Great thicknesses of Permian carbonate may have deposited as platforms atop oceanic plateaus, especially during the Middle Permian, when large fusulinids were important contributors to the volume of carbonate produced. A significant proportion of these organisms now found as fossils within the Cache Creek terrane, were endemic to the Tethyan realm, at the eastern margin of Pangea. In the Permian, the supercontinent extended from the south pole to within a few degrees of the north pole (Ross and Ross, 1985) resulting in extreme provinciality of low-latitude marine fauna, including fusulinids.

Permian time can also be considered the birthdate of the Cache Creek terrane. Rupture and initiation of subduction of Panthalassic ocean crust gave birth to the Cache Creek intra-oceanic arc. Oldest isotopically dated volcanic rocks attributed to this arc are ~263 Ma ignimbritic units in the French range near Dease Lake (Mihalynuk *et al.*, 2004). Oceanic strata offscraped during subduction at this arc produced an accretionary prism that comprises much of the Cache Creek terrane as we know it today. The arc component is called the Kutcho arc in northern British Columbia, where it is of particular importance because it includes the Kutcho Creek volcanogenic massive sulphide deposit. In the Atlin area, massive sulphide mineralization at the Joss’alun occurrence may be hosted by Kutcho-equivalent volcanic rocks (Mihalynuk, *et al.*, 2003b). Volcanic detritus containing zircons of only Latest Permian - earliest Triassic age accumulated to form what we have informally called the Hardluck formation. Yet the plutonic roots of the arc are nowhere in evidence near Hardluck Peaks, perhaps indicating deposition of the Hardluck formation at some distance from the arc axis, despite the proximal character of the conglomerate units with boulders reaching one metre or more in diameter. Volcanic-clastic rocks intercalated with the jumbled Hardluck formation have a chemical composition that resembles MORB in some respects, but they also displays some characters of an arc tholeiite. Rocks in the Marianas basin have similarly

variable chemical composition (e.g. Hawkins, *et al.*, 1990). We interpret the mafic volcanic rocks in the Joss'alun belt as deposited in an extending fore- or back-arc setting, like in the Marianas basin. Mantle rocks of the Nahlin body may have been exposed and serpentinized in this extensional environment as suggested by serpentinite pebbles in the Hardluck formation. Alternatively the Hardluck formation may have been deposited in piggy-back basins atop an accretionary complex that included minor slivers of ultra-mafic rocks which were eroded and redeposited.

By the Early Triassic, Pangea was beginning to break up, although it was not until the Early Jurassic that an equatorial seaway was established allowing east-west migration of fauna (e.g. Krobicki, 2003), resulting in loss of equatorial faunal provincialism. As Pangea break-up commenced, the Kutcho arc shut down. The reason for cessation of Kutcho volcanism is unknown. Perhaps the subduction zone was clogged with a carbonate-laden oceanic plateau, but it is questionable whether oceanic plateaus are buoyant enough to plug a subduction zone (e.g. Cloos, 1993), especially when the subducting lithosphere is likely to have been about 100 m.y. old (*i.e.* cold, dense and easily subducted). Lack of abundant ocean island basalt within the Cache Creek argues against plateau collision. Perhaps volcanism shut down because of a plate reconfiguration, or because of subduction zone hijacking by the neighbouring Stikine arc. Plate reconfigurations were likely during Pangea breakup, but this *ad hoc* explanation is difficult to test. Subduction zone hijacking is intriguing because a magmatic gap in the Stikine arc roughly corresponds with activity in the Kutcho arc, but the underlying cause remains at large. Whatever the cause, we tentatively ascribe a second phase of folding and thrust faulting in the accretionary complex to a local orogenic event at about this time.

Late in the Pliensbachian (late Early Jurassic ~186 Ma) Kutcho arc may have collided with the conjoined Quesnel and Stikine arcs (for a paleogeographic overview see Mihalynuk *et al.*, 1999; Mihalynuk *et al.*, in press). The Quesnel arc was driven up onto the miogeocline (Nixon *et al.*, 1993), and coeval, very rapid uplift was recorded by adjacent parts of Stikinia (Johnston, 1995) and widespread conglomerate blankets in the Whitehorse Trough (Johannson *et al.*, 1997). We speculate that this event produced a third set of folds (second set of folds that affect structures formed by the process of accretionary prism growth).

Subduction of oceanic crust was reestablished as evidenced by the presence of Early Jurassic radiolarian-bearing units within the accretionary complex as well as 174 Ma blueschist (Mihalynuk *et al.*, 2003, in press). The major segments of the Stikine and Quesnel arcs rotated into parallelism, entrapping relicts of Panthalassa oceanic crust and the Cache Creek terrane between them. Between 174 Ma and 172 Ma the two arc segments collided and northern Cache Creek terrane was emplaced southwestward over the Stikine arc segment. Emplacement structures include the major folds that deform Whitehorse Trough and Cache Creek strata; all are cut by the ~172 Ma plutons of the Fourth of July suite (Mihalynuk, 1999).

Only relatively minor brittle adjustments have effected the upper crust since ~172 Ma. One manifestation is a northwest-trending brittle fault zone that cuts the south-eastern margin of the Nakina River stock, and north-east-trending faults cut stratigraphy (Figure 2).

In Quaternary time, a lobe of continental glacier ice advanced up "Jos valley" transporting moraine that contained blocks of harzburgite as well as basalt/diorite with quartz-epidote-chalcopyrite-pyrite veins. Alpine glacier ice that persisted after retreat of the continental ice sheet were largely responsible for the present physiography as well as exhumation of copper sulphide mineralization in the upland areas, including the Joss'alun occurrence. This mineralization is now known to occur sporadically for at least 7.5 km along strike.

Conclusions

Four new copper sulphide showings within the belt of rocks containing the Joss'alun occurrence extend the limits of known mineralization to more than 7.5 km along strike. Analysis of mineralized samples of these vein occurrences, (NIC, Leefer, Moho Saddle, and Joeboy) show that some contain modest silver values, and that the sample from the Moho Saddle occurrence, contains nearly 1.5 g/t Au.

Imperial Metals Corporation carried out a diamond drill program at the Joss'alun occurrence in 2003. Two of the best intercepts were 17.75 m of 0.94% copper and 53.45 m of 0.34% copper (Robertson, 2003).

Major, minor and trace element composition of the volcanic rocks within the Joss'alun belt suggest a back- or forearc parentage, possibly analogous to the Marianas arc/back-arc system. Three phases of deformation within the belt include an episode of extension, possibly recording extension in the back- or forearc environment.

South of the Joss'alun belt, along the Nahlin fault, copper mineralization was found in a mafic volcanic unit informally named the Yeth Creek formation, and is herein called the "Yeth occurrence". These basaltic rocks have geochemical characteristics which are arc-like in many respects.

In all, five new copper showings were discovered within the area during the course of a ~3 weeks geological mapping program. Further prospecting and geological investigation is clearly warranted.

Acknowledgements

Operational funds for this project in 2003 were provided by Imperial Metals Corporation. Patrick McAndless, vice-president of exploration at Imperial Metals, is a major contributor to the success of this project through his unflinching and enthusiastic support. Dante Canil and Steve Johnston contributed substantially to this project by their mapping of the mantle rocks at Peridotite Peak and points southeast, and through stimulating discussions in the field. Norm Graham of Discovery Helicopters in Atlin, once again delivered flawless helicopter transportation. Able field assistance of Kyoko Nakano was made possible through the thoughtfulness of Gregg Dipple at The Univer-

sity of British Columbia. Rita Scott and Nora (Kuya) Minogue once again offered us refuge in their home in Atlin. Not least of all, thanks to the townsfolk of Atlin who continually support our field programs in many ways.

References Cited

- Aitken, J.D. (1959): Atlin map-area, British Columbia; *Geological Survey of Canada*, Memoir, 307, 89 pages.
- Ash, C.H. (1994): Origin and tectonic setting of ophiolitic ultramafic and related rocks in the Atlin area, British Columbia (NTS 104N); *B.C. Ministry of Energy, Mines and Petroleum Resources*, Bulletin, 94, 48 pages.
- BCMCM (1978): Atlin regional geochemical survey, 882 sites plus 160 lake sites; *BC Ministry of Energy and Mines* and the *Geological Survey of Canada*, RGS 51.
- Cloos, M. (1993): Lithospheric buoyancy and collisional orogenesis: Subduction of oceanic plateaus, continental margins, island arcs, spreading ridges, and seamounts; *Geological Society of America Bulletin*, Volume 105, pages 715-737.
- Dumont, R., Coyle, M. and Potvin, J. (2001): Aeromagnetic total field map British Columbia: Sloko River, NTS 104N/3; *Geological Survey of Canada*, Open File, 4093.
- English, J.M., Mihalynuk, M.G., Johnston, S.T. and Devine, F.A. (2002): Atlin TGI Part III: Geology and Petrochemistry of mafic rocks within the northern Cache Creek terrane and tectonic implications; in *Geological Fieldwork 2001, BC Ministry of Energy and Mines*, Paper 2002-1, pages 19-29.
- Hawkins, J.W., Lonsdale, P.F., Macdougall, J.D. and Volpe, A.M. (1990): Petrology of the axial ridge of the Mariana Trough backarc spreading center; *Earth and Planetary Science Letters*, Volume 100, pages 226-250.
- Jackaman, W. (2000): British Columbia Regional Geochemical Survey, NTS 104N/1 - Atlin; *BC Ministry of Energy and Mines*, BC RGS, 51.
- Johannson, G.G., Smith, P.L. and Gordey, S.P. (1997): Early Jurassic evolution of the northern Stikinian arc; evidence from the Labege Group, northwestern British Columbia; *Canadian Journal of Earth Sciences*, Volume 34, pages 1030-1057.
- Johnston, S.T. (1995): Stikinia and the Aishihik metamorphic suite; evidence of an arc-continent collision; in *Geological Society of America, Cordilleran Section, 91st annual meeting*; *Geological Society of America*, Volume 27, page 28.
- Krobicki, M. and Golonka, J. (2003): Onset of the Pangea breakup marked by the migration of Early Jurassic bivalves; *3rd Workshop of the IGCP Project 458, Triassic/Jurassic boundary changes, Stara' Lesna', Slovakia*, 28-30.
- Massey, N.W.D., MacIntyre, D.G. and Desjardins, P.J. (2003): Digital map of British Columbia: Tile NO10 (Northwest BC); *BC Ministry of Energy and Mines*, Geofile 2003-17.
- Mihalynuk, M.G. (1999): Geology and mineral resources of the Tagish Lake area (NTS 104M/ 8,9,10E, 15 and 104N/ 12W), northwestern British Columbia; *BC Ministry of Energy and Mines*, Bulletin 104, 217 pages.
- Mihalynuk, M.G. (2002): Geological setting and style of mineralization at the Joss' alun discovery, Atlin area, British Columbia; *BC Ministry of Energy and Mines*, Geofile, GF2002-6, 4 pages (plus digital presentation).
- Mihalynuk, M.G., Bellefontaine, K.A., Brown, D.A., Logan, J.M., Nelson, J.L., Legun, A.S. and Diakow, L.J. (1996): Geological compilation, northwest British Columbia (NTS 94E, L, M; 104F, G, H, I, J, K, L, M, N, O, P; 114J, O, P); *BC Ministry of Energy and Mines*, Open File 1996-11.
- Mihalynuk, M.G., Erdmer, P., Ghent, E.D., Archibald, D.A., Friedman, R.M., Cordey, F., Johannson, G.G. and Beanish, J. (1999): Age constraints for emplacement of the northern Cache Creek Terrane and implications of blueschist metamorphism; in *Geological Fieldwork, BC Ministry of Energy, Mines and Petroleum Resources*, Paper 1999-1, pages 127-142.
- Mihalynuk, M.G., Erdmer, P., Ghent, E.D., Archibald, D.A., Friedman, R.M., Cordey, F. and Johannson, G.G. (2004): Emplacement of French Range blueschist: Subduction to exhumation in less than 2.5 m.y.?; *Geological Society of America Bulletin*, in press.
- Mihalynuk, M.G., Johnston, S.T., Lowe, C., Cordey, F., English, J.M., Devine, F.A.M., Larson, K. and Merran, Y. (2002): Atlin TGI Part II: Preliminary results from the Atlin Targeted Geoscience Initiative, Nakina Area, Northwest British Columbia; in *Geological Fieldwork 2001, BC Ministry of Energy and Mines*, Paper 2002-1, pages 5-18.
- Mihalynuk, M.G., Johnston, S.T., English, J.M., Cordey, F., Villeneuve, M.J., Rui, L. and Orchard, M.J. (2003a): Atlin TGI Part II: Regional geology and mineralization of the Nakina area (NTS 104N/2W and 3); in *Geological Fieldwork, BC Ministry of Energy and Mines*, Paper 2003-1, pages 9-37.
- Mihalynuk, M.G. and Lowe, C. (2002): Atlin TGI, Part I: An introduction to the Atlin Targeted Geoscience Initiative; in *Geological Fieldwork 2001, BC Ministry of Energy and Mines*, Paper 2001-1, pages XX.
- Mihalynuk, M.G. and Peter, J.M. (2001): A hydrothermal origin for "crinkle chert" within the Big Salmon Complex; in *Geological Fieldwork 2000, BC Ministry of Energy and Mines*, Paper 2001-1, pages 83-84.
- Mihalynuk, M.G., Villeneuve, M.E. and Cordey, F. (2003b): Atlin TGI, Part III: Geological setting and style of mineralization at the Joss'alun occurrence, Atlin area (NTS 104N/2SW), MINFILE 104N136; in *Geological Fieldwork 2002, BC Ministry of Energy and Mines*, Paper 2003-1, pages 39-49.
- Monger, J.W.H. (1969): Stratigraphy and structure of Upper Paleozoic rocks, northeast Dease Lake map-area, British Columbia (104J); *Geological Survey of Canada*, Paper 68-48, 41 pages.
- Monger, J. (1975): Upper Paleozoic rocks of the Atlin Terrane, northwestern British Columbia and south-central Yukon; *Geological Survey of Canada*, Paper 74-47, 63 pages.
- Nixon, G.T., Archibald, D.A. and Heaman, L.M. (1993): ⁴⁰Ar-³⁹Ar and U-Pb geochronometry of the Polaris alaskan-type complex, British Columbia; precise timing of Quesnellia-North America interaction; in *Geological Association of Canada, Mineralogical Association of Canada*; annual meeting; program with abstracts; *Geological Association of Canada*, 1993, page 76.
- Robertson, S. (2003): Nak drilling hits long interval of copper mineralization; *Imperial Metals Corporation*, News Release, October 15, 2003, Vancouver, BC, page 30.
- Ross, C.A. and Ross, J.R.P. (1985): Carboniferous and Early Permian biogeography; *Geology*, Volume 13, pages 27-30.
- Souther, J.G. (1971): Geology and mineral deposits of the Tulsequah map area; *Geological Survey of Canada*, Memoir 362, 76 pages.
- Terry, J. (1977): Geology of the Nahlin ultramafic body, Atlin and Tulsequah map-areas, northwestern British Columbia; in *Current Research, Part A, Geological Survey of Canada*, pages 263-266.